HHS Public Access

Author manuscript

Curr Pharm Des. Author manuscript; available in PMC 2017 June 30.

Published in final edited form as:

Curr Pharm Des. 2015 ; 21(15): 1944–1959.

Smart Electrospun Nanofibers for Controlled Drug Release: Recent Advances and New Perspectives

Lin Weng and **Jingwei Xie***

Department of Pharmaceutical Sciences and Mary & Dick Holland Regenerative Medicine Program, University of Nebraska Medical Center, Omaha, Nebraska 68198, United States

Abstract

In biological systems, chemical molecules or ions often release upon certain conditions, at a specific location, and over a desired period of time. Electrospun nanofibers that undergo alterations in the physicochemical characteristics corresponding to environmental changes have gained considerable interest for various applications. Inspired by biological systems, therapeutic molecules have been integrated with these smart electrospun nanofibers, presenting activation-modulated or feedback-regulated control of drug release. Compared to other materials like smart hydrogels, environment-responsive nanofiber-based drug delivery systems are relatively new but possess incomparable advantages due to their greater permeability, which allows shorter response time and more precise control over the release rate. In this article, we review the mechanisms of various environmental parameters functioning as stimuli to tailor the release rates of smart electrospun nanofibers. We also illustrate several typical examples in specific applications. We conclude this article with a discussion on perspectives and future possibilities in this field.

Keywords

Electrospinning; Nanofibers; Controlled release; Drug delivery; Stimuli-responsive

INTRODUCTION

Electrospinning is a highly versatile and robust technique that produces fibers of diameters from several nanometers to tens of micrometers. Compared to other fiber fabricating techniques, such as wet chemistry methods and molecular beam lithography, it requires simpler apparatuses to operate but yields large quantities of products and employs a wide variety of polymers [1], semiconductors [2], ceramics [3], and oxides [4]. When the apparatuses and methodologies are carefully chosen, electrospinning can also generate core-sheath, porous, or hollow-structured nanofibers [5]. Recently, considerable progress has been made in the generation of smart nanofibers that are responsive to stimuli and undergo physical and/or chemical changes [6]. Such stimuli can include pH value, ionic strength, temperature, light, electric or magnetic fields, or combinations of these. In the present work,

*Address correspondence to this author at Department of Pharmaceutical Sciences and Mary & Dick Holland Regenerative Medicine Program, University of Nebraska Medical Center, Omaha, Nebraska 68198, United States; Tel: 402 559 9442; jingwei.xie@unmc.edu.

CONFLICT OF INTEREST

The authors confirm that this article content has no conflicts of interest.

we review highly interesting topics, including electrospinning, governed parameters for fabrication of electrospun nanofibers, biomedical applications of electrospun nanofibers, and stimuli-responsive electrospun nanofibers for controlled release. We mainly emphasize the principles of different types of smart nanofibers and highlight several typical examples in each case. In addition, we compare smart electrospun nanofibers to other well-established and environmentally responsive drug delivery vehicles with regard to their advantages and shortcomings.

ELECTROSPINNING

The first documented practice of the electrospraying phenomenon dates back to the 17th century, when William Gilbert observed that a water droplet close to an electrically charged amber formed a cone shape and small droplets were ejected from the tip [7]. By the end of the 19th century, there had been numerous mentions in literature of electrical spinning and its trial materials, include shellac, beeswax, sealing-wax, gutta-percha, and collodion [8]. The first patented electrospinning process appeared in 1900 [9]. Nevertheless, electrospinning was not fully explored for producing nanofibers until the early 1990s. Several research groups including Reneker [10–12] and Rutledge [13, 14] popularized the electrospinning technique, demonstrating many organic polymers can be electrospun into nanofibers. Since then, more and more efforts have been devoted to electrospinning.

An electrospinning setup usually consists of a power supply, a piece of feeding equipment, a spinneret, and a collector (Fig. 1). The feeding equipment typically contains a syringe pump and a syringe loaded with a solution. The high-voltage generator supplies tens of kilovolt to the spinneret, which is usually a syringe needle. The conductive collector, often a piece of aluminum foil, is grounded. A strong electric field forms between the spinneret and the collector, in which the charged solution in the spinneret has a strong tendency to move to the collector. A droplet of solution develops at the tip of spinneret, held by the surface tension of the stretched solution surface. This forms a Taylor cone. At the same time, a solution jet is ejected from the tip of the Taylor cone [15]. Along its trajectory to the collector, the volatile composition in the jet evaporates quickly, or the melt cools down swiftly. Both of these changes are due to the large surface area to volume ratio of the jet [10]. Extremely fine solid fiber is formed after the jet reaches the collector.

GOVERNING PARAMETERS OF ELCTRONSPINNING

Due to the complexity of electrospinning's principle, a variety of parameters can be tuned to govern the diameter, morphology, composition, structure, secondary structure, and alignment of the final product as shown in Figure 1. Table 1 summarizes the empirical operating parameters in controlling diameters, morphologies, and structures of fibers.

The flow rate Q determines the diameter of electrospun fibers to some extent because of its influence on the charge density. When the flow rate exceeds a critical value, the delivery rate of the solution jet to the capillary tip exceeds the rate at which the solution is removed from the tip by the electric force. This shift in the mass-balance results in a sustained but unstable jet and the formation of fibers with beaded structure [16].

The strength of the electrical field, which is determined by the applied high voltage V and the distance D between the spinneret and the collector, is pivotal to controlling the morphology of electrospun nanofibers. Given a certain distance, a higher voltage generally leads to a thinner diameter in the fibers, though there is a threshold above which a higher voltage may cause an irregular increase of the diameter [17]. Electric fields can also be used in more advanced setups, for instance, by using dual fields where the secondary electric field is perpendicular to the primary one [18]. Using this approach, the orientation of fibers on the collector can be well controlled, resulting in nicely aligned fibers.

The delicate balance between the surface tension and the electrical field determines the final morphology of fibers. Due to the poor conductivity of common polymers, charges accumulate on the surface of polymeric fibers and migrate to the collector upon the arrival of fibers. Thus, an increase in the voltage and reduction of the distance both prompt the formation of a beaded feature, which has the similar effect as varying flow rates Q [19]. The conductivity of the solution can also affect the fiber diameter distribution. A strong electrical field does not favor a highly conductive solution, which is unstable and leads to a broad diameter distribution [20]. However, attempts have been made to adjust the conductivity of the solution to achieve different purposes. For example, Cai *et al.* [21] added sodium dodecyl sulfate to zein and polyethylene glycol (PEG) solutions to increase the conductivity, which eventually made the obtained nanofibers in multiple orientations and form a loose and fluffy architecture.

Electrospinning can be viewed as a charged liquid jet moving downfield. The introduction of an electrostatic lens, uniquely designed collectors, or external magnetic fields will exert either Coulomb force or Lorentz force on the jet and change its trajectory to the collector. Huang *et al.* [22] showed selective deposition of electrospun nanofibers using an electrostatic lens. Li *et al.* [23] have used a collector consisting of two pieces of electrically conductive substrate separated by a gap, the width of which can reach several centimeters, for the fabrication of uniaxially aligned nanofiber arrays. Matthew *et al.* [24] demonstrated a simple and highly successful method for spinning a sheet of aligned nanofibers by using a grounded rotating mandrel. Xie *et al.* [25] invented radially aligned poly(ε-caprolactone) (PCL) nanofibers by utilizing a specially designed collector composed of a central point electrode and a peripheral ring electrode. In addition, studies have demonstrated the formation of aligned nanofiber arrays between two magnet bars placed above the collector, which is independent on the incorporation of magnetic nanoparticles to nanofibers [26, 27].

The rate of solvent evaporation from the liquid jet could create secondary structures on fibers and determine the uniformity of electrospun fibers. A highly volatile solvent absorbs heat from the jet, lowering the temperature of the liquid jet, and decreases the thermodynamic stability of the non-solvent phase. Thermally induced phase separation (TIPS) occurs in the non-solvent rich phase and non-solvent lean phase. The concentrated phase solidifies shortly after phase separation and forms the matrix, whereas the lean phase forms the pores [28]. A high humidity may also bring porous structures to electrospun fibers attributed to vapor-induced phase separation, TIPS, and/or breath figures when the solvent is volatile without containing any water. Humidity ϕ controls the evaporation rate of the fluid jet when the water is used as a solvent component. A high relative humidity suppresses the

evaporation rate, which allows the charged jet to continue to elongate. Meanwhile, the surface area of the jet increases, and the charge per unit area on the surface of the jet decreases, resulting in the capillary instability. Beaded fibers were observed when the relative humidity was higher than 52.6% during electrospinning [29].

ELECTROSPUN NANOFIBERS IN BIOMEDICAL RESEARCH

Electrospun nanofiber scaffolds often possess interconnecting pores to allow cells to attach, migrate/infiltrate, and proliferate, while permitting free exchange of nutrients and wastes [30]. Their inherently high surface-to-volume ratio enhances cell attachment, drug loading, and mass transfer properties [1]. The surface can be modified with bioactive molecules and cell recognizable ligands capable of imitating the natural extracellular matrix (ECM). They also show suitable mechanical properties to maintain the frame, and they can be biocompatible and biodegradable. We credit broad applications of electrospun nanofibers in the biomedical area to these advantages (Fig. 2).

Regenerative medicine is an interdisciplinary field combining life science and engineering. The final goal is to grow man-made tissues to replace the ones destroyed by diseases, accidents, or congenital defects without triggering severe immune response [31]. Scaffolds play an important role in regenerative medicine as they can act as not only a substrate for supporting cell growth, forming certain structures, or regulating cell behaviors but also as a sustained local delivery system for growth factors and/or signaling molecules and the enhancement of cell functions and tissue regeneration. Electrospinning offers a cost-effective method for fabricating nanofiber scaffolds to mimic native ECM composed of an interlocking mesh of proteins and glycosaminoglycans. PCL, poly(lactic acid) (PLA), poly(glycolic acid) (PGA), poly(lactic-*co*-glycolic acid) (PLGA) and poly(lactic acid-*co*-caprolactone) (PLCL) are the most popular raw materials due to their ease of processing, stable mechanical properties, and good biocompatibility [32–36]. Natural polymers, such as collagen, gelatin, chitosan, and silk fibroin have also been electrospun into nanofiber scaffolds [24, 37–39]. In addition, various materials and bioactive molecules have been encapsulated in polymers by co-electrospinning [40] or emulsion electrospinning [41] to help develop diverse chemical, structural, and mechanical properties. An alternative method is to modify the surface of nanofibers with proteins or peptides [42]. Other than the modulation of compositions, topographic cues rendered by electrospun nanofibers demonstrated the control of cell behaviors [43–45]. Besides, electrospun nanofibers showed the promise of local delivery of growth factors or signaling molecules for tissue regeneration [46–48].

The ideal wound dressings should be multi-functional: fighting against acute or chronic infection; maintaining a balanced moisture and gas exchange environment; absorbing extrudates and blood from wounds; and promoting cell proliferation and migration and, thus, wound healing [49–52]. Electrospun nanofibers as wound dressings could simultaneously present all these features. The small pore size of electrospun nanofiber dressings, below 1 μm, protects the wound from bacterial penetration via aerosol particle capturing mechanisms, while allowing O_2 permeability [49]. The antibacterial substances, such as Ag nanoparticles [53], iodine [54], and mupirocin [55], have been added to nanofiber dressings

to eliminate infections. Growth factors [56], vitamins [57], and minerals [58], as active compounds in wound healing, have been incorporated into nanofibers to promote normal skin growth and to reduce scar tissue formation. Nanofiber dressings seem capable of simultaneously preventing infection and fostering cell proliferation and migration/wound healing by incorporation of multiple agents and control of pore size.

The intrinsically large surface, specific area, tunability over a 3D fine structure, and diversity of materials nominate electrospun nanofibers as an ideal candidate for the construction of biosensors that detect gases [59–62], ions [63, 64], or biomolecules [65–67]. Recent studies have demonstrated that a biosensor made of electrospun nanofibers is even capable of detecting circulating tumor cells (CTC) [68]. For example, Tseng's group developed "NanoVelcro" chips that can identify and isolate single-CTC by conjugating streptavidin and biotinylated capture agents to electrospun PLGA nanofibers [69, 70].

Electrospun nanofibers have been used as a vehicle for local drug delivery due to the ease of encapsulation of chemical and biological molecules during electrospinning process. In applications of electrospun nanofibers in regenerative medicine and wound dressings, therapeutic agents are often incorporated to the nanofibers for controlled release. In this article, we mainly focus on reviewing smart electrospun nanofibers for controlled release.

STIMULI-RESPONSIVE ELECTROSPUN NANOFIBERS FOR CONTROLLED RELEASE

The ideal nanofiber formulations for drug delivery to patients should be spatially and temporally controlled. Nanofibers are often administrated in a dosage form via a local delivery route. Thus, the release of drugs occurs only at the targeted site, avoiding systematic exposure of the drugs. The spatial control of drug delivery can be readily realized by placing electrospun nanofibers at the targeted site through invasive or non-invasive means. In earlier studies, the temporal control of drug release from electrospun nanofibers has been mainly determined by drug diffusion rates, drug dissolution rates, drug physical desorption rates, diameters of fibers (lengths of diffusion barrier), and/or polymer degradation/erosion rates [17, 71–75]. Recent efforts have been devoted to development of activation and feedback factors electrospun nanofibers to initiate the release and/or regulate the release rate of drugs over time. Such nanofibers are also called smart electrospun nanofibers [76–78] as a component undergoing physicochemical changes is usually present in this activation-modulated or feedback-regulated system. This system is automatically responsive to changes in environmental parameters including pH value, temperature, light, electrical field, and magnetic field, which can tailor the drug release rate based on the prognostic markers.

i. pH Responsive Electrospun Nanofibers

The human body is regulated by acid-base homeostasis, which keeps the pH of the arterial blood between 7.38 and 7.42. Nevertheless, many tissues or cell compartments have their own distinctive pH environments for normal functioning. For example, the pH of gastric acid is 1.5–3.5, 4.5–5.0 for lysosomes [79], and 8.0 for pancreas secretions [80]. A decrease in

the local pH has been frequently associated with inflammation [81], tumor growth [82], and myocardial ischemia [83], which is the result of the presence of short-chain, fatty acid by-products of bacterial metabolism, glycolytic activity of infiltrated neutrophils, or overproduction of lactic acid. A change in the pH of the wound also indicates the progress of wound healing [84]. Thus, the pH is one of first and most studied stimuli to trigger and modulate the release of drugs. An ideal scenario is that the pH-responsive, drug-loaded electrospun nanofibers (pH-RDLEF) release at the characteristic pH of the disease, and when the condition is improved and the pH shifts to the normal value, such nanofibers could reduce the release rate or completely cease the release.

There exists more than one mechanism that enables pH-RDLEF to function (Fig. 3). But pH-RDLEF having a simple irreversible one-time release and reversible multiple-time release characteristics is related to the same phenomena of swelling. Polymers containing carboxylic acids (Fig. 3A) or amine groups (Fig. 3B) are the most extensively used pH sensitive polymers. They end up in protonation or deprotonation, associated with changes in hydrophilicity and morphology, when placed in different pH environments. This phenomenon has been comprehensively exploited in the pH-sensitive hydrogels [85–87]. The same concept has been extended to electrospun nanofibers. Cao *et al.* [88] prepared pH-sensitive poly[styrene-*co*-(maleic sodium anhydride)] (PSMA) and PSMA-cellulose acetate (CA) composite nanofibers and then cross-linked and converted them into hydrogel nanofibers in the presence of diethylene glycol. It was found that these nanofibers possessed better mechanical strength than classic cast hydrogels and displayed a pH-dependent swelling when immersed in water. Qi *et al.* [89] demonstrated the acceleration of the release rate of a model drug, paracetamol, from pH-RDLEF having ortho ester groups in mildly acidic conditions as these nanofibers are stable at pH=7.4 but degrade at lower pH (e.g., 4.0 and 5.6). In a separate study, Cui *et al.* [90] introduced low-pH sensitive acetal groups into the poly(ethylene glycol)-poly($_{D,L}$-lactide) (PELA), which led to the swelling of the co-polymer at lower pH (Fig. 4) and acceleration of the release rate of paracetamol from the nanofibers. The pH value can be a factor to trigger the release (Fig. 3C). Yun *et al.* [91] demonstrated a simple way to control the release of ibuprofen from acid-responsive electrospun nanofiber scaffolds for skin wound healing. They designed a system that automatically started to release ibuprofen when the environmental pH was below 7.4, targeting the acidic bacterial infection site. Electrospun poly($_{L}$-lactide) (PLLA) nanofibers, incorporated with $NaHCO_3$, started to decompose and to generate CO_2 when pH was low. *In vitro* release tests showed the pH-RDLEF swelled slightly after incubation at pH=5.0 for 48 h but maintained the 3D fibrous structure. Under the same conditions, the percentages of cumulative release of ibuprofen are 78.2% and 30.6% pH-RDLEF and the controlled group without addition of $NaHCO_3$. Further *in vivo* tests showed that the acid-responsive, ibuprofen-loaded electrospun nanofibers can minimize the inflammation in the early stage. A reduced response time for this pH-RDLEF can be achieved by treating PLLA nanofibers with air-plasma, which makes the surface of PLLA nanofibers hydrophilic and enables H^+ to access $NaHCO_3$ in the fibers more easily [92]. The air-plasma treatment is also an alternative method for introducing pH-sensitive groups to electrospun nanofibers. The air-plasma treatment to PCL and PLA nanofibers can generate carbonyl, carboxyl, and hydroxyl groups on their surfaces [93, 94]. Based on this finding, Jiang *et al.* [95] proposed that air-

plasma treated PCL or PLA nanofibers coated with polydopamine could be pH-responsive. It was demonstrated that a mussel-inspired protein polydopamine coating, serving as a mediator, can tune the loading and release rate of charged molecules from electrospun PCL nanofibers in solutions with different pH values (Fig. 5A–D). The viability of cancer cells after treatment with doxorubicin-released media at different pH values indicated that the media containing doxorubicin released in solutions at low pH values could kill a significantly higher number of cells than those released in solutions at high pH values (Fig. 5E–F). Though the pH-responsive nanofiber systems have been demonstrated successfully for the controlled release of small molecular drugs, such systems may not be suitable for regulating release of proteins as the change of pH values could cause denaturation of proteins.

ii. Thermoresponsive Electrospun Nanofibers

Human body temperature falls into a narrow range and experiences minor fluctuations during the day. Deviations from normothermia can include fever, hyperthermia, or hypothermia. Among them, fever is a symptom of many medical problems, including infectious disease [96], immunological disease [97], cancers [98], and metabolic disorder [99]. External sources can be applied to heat up or cool down tissues, thus inducing localized hyperthermia or hypothermia. This suggests that temperature can be manipulated and used as a stimulus to modulate the drug release. Temperature-responsive drug-loaded electrospun nanofibers (T-RDLEF) have earned their place among “smart” electrospun fibers as the drug release rate can be programmed according to the circadian rhythm of the disease being treated. T-RDLEF is made from polymers that undergo abrupt changes in solubility, in other words, the affinity of water. This is the result of competition between hydrophilic and hydrophobic moieties on the polymer chain [100, 101]. The balance point is called the lower critical solution temperature (LCST), at which the polymer neither favors hydrogen bonding with the polymer nor with water [102].

Among temperature sensitive polymers (Table 2), PNIPAAm, PDEA, PVCL, and PMVE have been widely explored as components of thermoresponsive system because their LCSTs are close to normothermia. PNIPAAm was proposed earliest and is most frequently used in the form of hydrogel (Fig. 6). It has also been processed into electrospun nanofibers for temperature-controlled drug delivery. The electrospun PNIPAAm fiber mat was first reported by Rockwood *et al.* [110]. They demonstrated the feasibility of fabrication of PNIPAAm nanofibers and the control over the diameter of fibers by electrospinning. No change in the chemical structure of PNIPAAm during the electrospinning process was confirmed by Raman spectroscopy and FT-IR. The PNIPAAm fiber mat is soluble in water when the temperature is below LCST; however, it loses its fibrous feature at temperatures above LCST as well. Inspired by Rockwood’s work, different methods have been developed to circumvent this obstacle that kept PNIPAAm from practical applications. Among them, the use of copolymer is a promising way to address this issue. Okuzaki *et al.* [111] synthesized poly(N-isopropylacrylamide-*co*-stearyl acrylate) (P(NIPAAm-*co*-SA)) having the LCST of 23 °C, lower than that of PNIPAAm due to incorporation of hydrophobic stearyl acrylate monomers. They further fabricated P(NIPAAm-*co*-SA) nanofiber mats using electrospinning. The time-dependent deswelling and swelling of P(NIPAAm-*co*-SA)

nanofiber mats was reversible and reproducible. It suggested that the rapid thermo-responsive volume changes of P(NIPAAm-*co*-SA) nanofiber mats could be attributed to the large specific surface area of the mats. Kim *et al.* [112] fabricated electrospun poly(N-isopropylacrylamide-*co*-N-hydroxymethylacrylamide) (P(NIPAAm-*co*-HMAAM)) nanofibers as reversible T-RDLEF (Fig. 7A). The synthesized nanofibers had an average diameter of 600–700 nm (Fig. 7B1–B2). The methylol group can be chemically cross-linked by self-condensation upon heating, resulting in reduction of the aqueous solubility of the copolymer and maintenance of the fibrous feature [113]. Contrary to Okuzaki's work, the increased percentage of hydroxymethylacrylamide in the copolymer led to the rise in LCST of P(NIPAAm-*co*-HMAAM) from 33 °C to 40 °C, which was because of increased hydrophilic hydroxyl groups. The thermal deswelling test showed the reversibility and reproducibility of deswelling and swelling and P(NIPAAm-*co*-HMAAM) nanofibers reached full deswelling in one minute (Fig. 7C). Dextran-loaded T-RDLEF was also prepared by electrospinning the copolymers blended with fluorescein isothiocyanate (FITC)-dextran (Fig. 7D). The cross-linked nanofibers demonstrated "on–off" switchable release of FITC-dextran. The release of dextran from nanofibers was mainly caused by its being squeezed out of the collapsing polymer network [114]. In contrary, the release of dextran ceased upon cooling because of the suppressed diffusion of the FITC-dextran molecules. However, they only demonstrated the release profiles at the temperatures of 10 °C and 45 °C that are far beyond human body temperature. An in vitro experiment conducted at a temperature of 35–42 °C may be able to reveal the actual response of this T-RDLEF *in vivo*.

Alternatively, the co-electrospun technique can also overcome the barrier of high aqueous solubility of PNIPAAm. Polystyrene (PS) [115–117], PCL [118, 119], poly(2-acrylamido-2-methylpropanesulfonic acid) [120], poly (ethylene oxide) (PEO) [121], and PLCL [122] have been co-electrospun with PNIPAAm to achieve a thermal-responsive effect. Many of them are considered biocompatible and biodegradable, which makes them excellent candidates for controlled release.

iii. Light Responsive Electrospun Nanofibers

Human bodies are often exposed to light (e.g., sunlight and artificial light). The wavelength of light encountered in daily life ranges from 3000 nm of the infrared heater to 315 nm of ultra-violet light A (UVA) in sunlight. Below 315 nm, the ultra-violet (UV) light is not suitable for therapeutic purposes since the high-energy photons start to damage DNA directly [123]. Light-responsive drug-loaded electrospun nanofibers (L-RDLEF) have attracted much attention because of their fast response [124] and avoidance of chemical stimulants and byproducts [125]. For safety considerations, L-RDLEF should be able to respond to light with a wavelength longer than 315 nm, and if possible, L-RDLEF should be restorable to its original state by other stimuli.

Photoisomerization paves the way for L-RDLEF, which has been utilized for rewriteable optical data storage and molecular devices [126–128]. There are two major classes of photoisomerization behaviors, including open-closed ring transition and cis-trans conversion, which have been used in the light-responsive electrospun nanofibers. The most representative example of the open-closed ring transition is spiropyran (SP) and its

derivatives. Sousa *et al.* [129] showed the fabrication of electrospun poly(methacrylic acid) nanofibers and further covalently modified the nanofibers with SP or cyclodextrin-SP inclusion complex. The photo-reversibility of the nanofibers was verified by recurrent exposure to visible and UV light and measuring water contact angles on the surface. The same result was also found in the azobenzene (azo) modified polymers that underwent reversible photoisomerization between its cis and trans forms at different wavelengths. Chen *et al.* [130] modified the electrospun PCL nanofibers with azo upon a facile one-pot reaction (Fig. 8A). The change of wettability of the fibers was large, reversible, and light-responsive, confirmed by UV-vis spectroscopy and contact angle measurements (Fig. 8B). Meanwhile, they found that the change in contact angles during the photoisomerization is positively correlated to the amount of azo added to PCL during electrospinning. They assumed that such changes in wettability arose not only from the azo surface functionalization but also from the roughness intrinsically offered by the electrospun nano/microscale hierarchical structures. Interestingly, the only existing drug-release experiment of L-RDLEF was published by Fu *et al.* [131], two years ahead of Sousa [129] and Chen [130]. They fabricated poly(vinylbenzyl chloride -glycidyl methacrylate) (PVBC-*b*-PGMA) nanofibers by electrospinning (Fig. 9A). The nanofibers were then cross-linked by azo molecules via azido groups. A prodrug, α-cyclodextrin-5-fluorouracial (α-CD-5FU), can attach to the modified PVBC-*b*-PGMA-azo when azo groups were in the trans configuration but not in the cis configuration induced by UV light. The exposure of the L-RDLEF to UV light led to a slight swelling of nanofibers (Fig. 9B) and well-controlled release of α-CD-5FU (Fig. 9C). There was no drug release at all when the fibers were immersed in water for 1 h in the dark, while maximal drug release was observed after 30 min of UV exposure. By exposing the fibers to several “UV light intervals” interspersed by periods when the fibers were placed in the dark, it was clearly shown that drug release only occurred upon UV exposure. This design utilized a guest-host interaction between azo and cyclodextrins, thus limiting the choice of drugs as it required them to be chemically modified to bind to hydroxyl group of cyclodextrins [132]. A better design is to replace the monomer of cyclodextrins with their dimers, which contains two different types of cyclodextrins [133]. By carefully choosing the azo group and exploiting different affinities of cyclodextrins to azo [134], one cyclodextrin may selectively bind to the azo group, which could be used for controlled release triggered by photons [135].

The progress is encouraging, but the drawbacks of current L-RDLEF should be addressed as well. The UVA penetration depth in tissue is limited, and it has been shown to inflict indirect DNA damage [136]. Recently, near infrared-sensitive nanoparticles have gained much attention for photothermal therapy and drug delivery due to the deeper penetration and no side effects to the tissue of near infrared light [137–139]. More efforts should be devoted to the use of a combination of near infrared-sensitive nanoparticles and thermo-sensitive polymers for producing L-RDLEF.

iv. Electric Field Responsive Electrospun Nanofibers

An electric field influences the swelling behavior of electric field responsive polymers [140–143]. Based on the mechanisms, electric field responsive polymers are mainly classified into the following categories: electroactive polymers, ion-doped conducting polymers, and

polymer composites/bends/coatings [144]. Electroactive polymers (e.g., piezoelectric polymers, electrostrictive, and dielectric elastomers) display a change in their size or shape when stimulated by an electric field, which have not been investigated for controlled release by an electric field [145, 146]. Ion transport takes place in conducting polymers during the electro- and/or chemical oxidation and reduction. The reversible intercalation motion of the ions results in a volume change of conducting polymers. The polymeric nanofibers incorporated with carbon nanotubes operating in electrolyte can lead to volume changes because of capacitive charging [147]. Both conducting polymer coated electrospun nanofibers and carbon nanotube encapsulated electrospun nanofibers have been examined for controlled release under electrical stimulation.

Abidian *et al.* [148] fabricated poly(3,4-ethylenedioxythiophene) (PEDOT) coated PLGA core-sheath nanofibers and demonstrated the controlled release by electric fields. They used electrospun PLGA fibers as a template, coated the fibers with PEDOT (Fig. 10A1–A2). They further confirmed the PEDOT coating by dissolving the PLGA with dichloromethane (DCM) to form PEDOT nanotubes (Fig. 10A3–A4). They demonstrated a controlled release of an anti-inflammatory drug, dexamethasone (DEX), from PEDOT-coated PLGA nanofibers using an electrical stimulation (Fig. 10B). The drug loaded PEDOT-coated PLGA nanofibers were actuated by applying a positive voltage of 1V with scan rate of 0.1 V/s for 10 s at five specific times, and each of which led to a stage of enhanced DEX release. The result was attributed to the contraction force [149] formed during the shrinkage of PEDOT coating as negatively charged counterions were expelled towards the solution to maintain overall charge neutrality when applying a positive voltage (Fig. 10C–D). This hydrodynamic force inside the core-sheath nanofibers caused major DEX release through topological openings on PEDOT coatings. The release rate under stimulation was lower than that from PLGA nanofibers, but higher than that from PEDOT-PLGA core-sheath nanofibers without applying an electrical stimulation (Fig. 10E–H).

Carbon nanotubes, which are electrically conductive, have been regarded as potential molecular quantum wires. Yun *et al.* [150] dispersed carbon nanotubes in polymers to make the polymer conductive without introducing the cytotoxicity of carbon nanotubes [151]. They prepared the electro-responsive transdermal drug delivery system composed of electrospun polyvinyl alcohol (PVA)/poly(acrylic acid) (PAA)/multi-walled carbon nanotubes (MWCNTs) nanocomposites (Fig. 11A–B). They applied oxyfluorination to the hydrophobic MWCNTs' surface to increase interfacial adhesion forces between MWCNTs and polymers, which led to a better dispersion of MWCNTs and determined the swelling and drug release characteristics of nanofibers. The swelling rate and ratio of nanofibers positively correlated to the applied voltages (Fig. 11C). Further investigations revealed that the drug release from nanofibers was dependent on applied electric voltages (Fig. 11D). The drug release rate from nanofibers increased with increasing applied voltages. Though the authors did not explain this relationship, it appears that swelling behavior of nanofibers allows a higher permeability of loaded drug, which is quite similar to the T-RDLEF.

Both examples prompt the development of practical T-RDLEF that can be incorporated to neural prostheses for delivery of drugs, growth factors, neurotransmitters or anti-neurodegenerative molecules to the nervous system. The local field potential could be used

to monitor the tissue response and simultaneously function as a trigger to release drug molecules when it is abnormal upon occurrence of disorders.

v. Magnetic Field Responsive Electrospun Nanofibers

Substantial interests in magnetic materials have been devoted to their potential biomedical applications. As a stimulus, the magnetic field has unmatchable advantages over other options. Living tissues are magnetically transparent since their compositions are mainly water, which is diamagnetic and negligibly repelled even in a powerful magnetic field, like a clinical magnetic resonance imaging machine [152], while applied light or heat can only reach up to four inches beneath the skin [153]. In addition, the human body is able to tolerate a magnetic field of high strength. Humans can tolerate magnetic fields of up to 7 Tesla [154], while a strong light or heat source usually leads to DNA damage and cell death.

In order to generate magnetically responsive fibers, superparamagnetic nanoparticles (SPNs) have been incorporated into polymers during electrospinning [155–157]. Superparamagnetism appears in small ferromagnetic or ferrimagnetic nanoparticles that randomly flip their magnetization direction under the influence of temperatures [158]. This property guarantees SPNs to be aligned with the applied alternating current magnetic field (ACMF) without showing magnetic hysteresis that is not desirable by the magnetic field-responsive drug-loaded electrospun nanofibers (MF-RDLEF) [6]. Such practices have extensively used Fe-based magnetic nanomaterials, like Fe_3O_4 (magnetite) or Fe_2O_3 (maghemite), because of their low cytotoxicity and high biocompatibility [159, 160]. Wang *et al.* [155] PAA-coated Fe_3O_4 nanoparticles loaded PEO and PVA fibers by electrospinning, exhibiting superparamagnetic properties and showed a magnetic field strength correlated deflection toward an external magnetic field.

SPNs have been used in attempts to create MF-RDLEF. Tan *et al.* [156] incorporated ammonium oleate-capped Fe_3O_4 nanoparticles (5–10 nm in diameter) to poly (hydroxyethyl methacrylate) or PLLA nanofibers during electrospinning. The nanofibers were superparamagnetic without showing magnetic hysteresis based on the magnetization curves, which was consistent with Fe_3O_4 nanoparticles. An albumin with dog fluorescein isothiocyanate (ADFI) was added to the nanofibers as a model drug. About 1% ADFI was released from nanofibers in 24 h. In a similar study, Wang *et al.* [161] added Fe_3O_4 nanoparticles and drugs (e.g., indomethacin and aspirin) to electrospun dehydroxypropyl methyl cellulose phthalate and CA nanofibers. The presence of Fe_3O_4 nanoparticles had no influence on the release profiles, though it was possible to move nanofibers to the target site under the guidance of an external magnetic field. Recently, Savva *et al.* [162] took a step further in systematically examining the drug release from MF-RDLEF(Fig. 12A). They electrospun 5 nm oleic acid (OA)-coated Fe_3O_4 (OA-Fe_3O_4) with PEO (hydrophilic, thermoresponsive) and PLLA (hydrophobic) to form continuous fibers of approximately 2 μm in diameter, loaded with N-acetyl-p-aminophenol (acetaminophen) as a model drug (Fig. 12B). They evaluated the MF-RDLEF's heating ability under ACMF and found that an increase in the temperature of MF-RDLEF was proportional to the wt% of the loaded OA-Fe_3O_4 (Fig. 12C). However, they did not present magnetothermally triggered release data, which is crucial to demonstrate the possibility of MF-RDLEF. Instead, they showed the drug

release profiles in the form of acetaminophen absorption for PEO/PLLA/acetaminophen (Fig. 12D), PEO/PLLA/20 wt% OA-Fe_3O_4 and PEO/PLLA/70 wt% OA-Fe_3O_4 acetaminophen containing 20 and 70 wt% OA-Fe_3O_4, and concluded that the differences between the drug release rates were due to the varied amounts of OA in the electrospun nanofibers, which was hydrophobic and reduced the contact of the nanofibers with surrounding water. These studies examined the drug release from MF-RDLEF; however, no studies have reported the control of drug release from MF-RDLEF by applying an external magnetic field.

The drug release from MF-RDLEF could be guided by magnetic hyperthermia, a phenomenon that describes the movement of SPNs under the influence of an external ACMF [163]. The applied field heats SPNs embedded in nanofibers because of Néel relaxation [164]. The SPNs would be heated up as long as they are below the Curie temperature, and the heating would stop when SPNs reach the Curie temperature and lose their superparamagnetism, as the Curie temperature of SPNs provides a fail-safe mechanism [165]. The Curie temperature is determined by judicious selection of compositions and sizes of particles. Hyperthermia can be precisely controlled to prevent the occurrence of overheating. However, to date, no studies have clearly shown a stage drug release from MF-RDLEF by applying an external magnetic field. If the polymer used is a thermo-responsive polymer (e.g., PNIPAAm), the nanofibers periodical exposure to ACMF may lead to the deswelling and swelling cycle of PNIPAAm, which could thus result in the control of release based on the similar mechanism as T-RDLEF.

vi. Multiple Stimuli Responsive Electrospun Nanofibers

Multi stimuli-responsive electrospun fiber systems that respond to a combination of two or more signals have been developed to extend the already broad tunability over the drug delivery. These combined responses can occur at the same time or in a sequential way. For instance, dual stimuli-responsive drug-loaded Electrospun nanofibers can activate the release of drugs to an infection site whenever the local pH or temperature shifts from the normal value. Multi stimuli-responsive electrospun nanofiber systems can be a collective body of a few single stimuli-responsive electrospun fibers, but it can also be made of macromolecules or polymer mixtures/blends or surface coating that respond to multiple stimuli.

Studies demonstrated the fabrication and swelling characterization of dual stimuli-responsive electrospun fibers. Chen and Hsieh [166] generated electrospun nanofibers composed of PNIPAAm/PVA blends responsive to both temperature and pH. At room temperature and at a pH below 4, the fibers showed nearly no swelling, whereas at room temperature and at a pH above 4 a high degree of swelling was observed. In contrast, at pH above 4 and at elevated temperatures (e.g., 70 °C) the swelling ratio was reduced from 15 to 2.6-fold. In a different study, Hsieh *et al.* [167] developed electrospun fiber films made of PAA/PVA blends and performed cross-linking by heating them to 140 °C. They investigated the swelling behavior of the fibers upon exposure to aqueous solutions of different pH values. A pronounced three-dimensional swelling occurred at pH values of between 4 and 7. The volume increased with increasing pH values. Interestingly, after exposure to an electric field, the swelling ratios further increased from 11 to 20-fold at pH = 4, which suggested

that the pH-dependent swelling of these films can be further augmented by the application of an electric field. In another study, Liu *et al.* [168] produced electrospun acrylamide/maleic acid (P(AM-MA)) nanofiber membranes sensitive to both ionic strength and pH. They first fabricated P(AM-MA) nanofibers with a diameter of 120 nm and performed crosslinking with diethylene glycol at 145 °C. The authors assumed that P(AM-MA) had a two-step dissociation to poly(maleic acid) whose pK_{a1} is 3.2 and pK_{a2} is 8.1 at room temperature. Upon an increase in ionic strength, the swelling ratios of the hydrogel reduced from 8 or 18-fold in water to 4 or 6-fold in a solution of ionic strength of 2.0 mol/dm^3. Upon increasing the pH, the swelling of the fibers showed a dual transition between pH 2.5 and 4.6, and the swelling ratio increased from 3- to 4-fold, then leveled off up to pH 8.5. After this, a second significant increase was noted from pH 8.5 to 11. Thus, the swelling behavior of P(AM-MA) fibers was subjected to both ionic strength and pH. Further studies demonstrated the control of drug release using multi-responsive electrospun nanofibers. Chunder *et al.* [169] fabricated PAA/poly(allylamine hydrochloride) (PAH) ultrathin fibers and incorporated cationic methylene blue (MB) as a model drug. PAA and PAH are both weak polyelectrolytes and carry opposite charges. No release of MB was observed at a pH value of 7 or higher since cationic MB molecules bonded tightly to anionic carboxylate groups on PAA. At a pH of 6 or lower, MB detached from PAA and released into the solution medium as some carboxylate groups on PAA were protonated. Further coating of PNIPAAm rendered PAA/PAH fibers a temperature-dependent drug release. A nearly 10-fold increase in release rates was observed at 40 °C than at 25 °C. These studies demonstrated the potential for combining multiple stimuli in electrospun nanofibers for controlled release. The associated difficulties for the development of such systems could include synthesis of the polymers that can degrade and respond to multiple stimuli under physiological conditions and achievement of a desirable combination of multiple stimuli.

CONCLUSIONS AND PERSPECTIVES

When comparing the published literature on smart electrospun nanofibers to that of other smart materials (e.g., hydrogels [170, 171] and nanoparticles [172, 173]), electrospun nanofibers cannot match them in either the total number of publications or how far it has gone in clinical trials [77]. What causes this difference? We do not agree that smart electrospun nanofibers are not as promising as previously believed. Bringing stimuli-responsive drug-delivery systems from the bench to the bedside is not a straightforward process. It took 11 years for thermoresponsive smart nanoparticles to move from preclinical research [174] to phase III clinical research [175], and hydrogels are still in pre-clinical research.

All smart materials face the same developmental challenges: the sophisticated designs complicate manufacturing process, reproducibility, and quality control; potential cytotoxicity *in vivo* is not fully understood; endogenous stimuli may differ from one person to another, imposing difficulties to creating a standardized commercial product; both tissue-penetration depth and the focusing of smart materials are questionable. Intrinsically, electrospun nanofibers offer multiple solutions to overcome these challenges if given sustained effort and enough time. For drug delivery, the high surface to volume ratio is the major advantage of

electrospun nanofibers, which greatly enhance their response rate to external stimuli, rendering discrete variations in response to the specific stimulus.

The smart materials could be complementary to each other since each of them has their distinctive physical and chemical properties. Nanoparticles are highly maneuverable and they are often administered via injection [176–179]. The response is fast but frequent injections (e.g., insulin for diabetes) compromise the appliance of patients [180]. Also, nanoparticles lacks the capability in forming a scaffold to support the tissue regeneration. Hydrogels may be administered via injection or implantation. However, they are suffering from poor mechanical properties. Smart electrospun nanofibers possess the similar properties as the fibers that are not responsive to external stimuli, capable of serving as a scaffold for tissue regeneration due to their biomimicry and good mechanical properties [181]. And simultaneously the release of signaling molecules can be controlled via different stimuli. Smart electrospun nanofibers may find applications in unique niches other than surgical implants such as transdermal drug delivery (e.g., direct placement on the skin) [182, 183], oral drug delivery [184], and vaginal drug delivery etc. [185]. In addition, smart nanoparticles, hydrogels, and nanofibers can be combined to form a composite/hybrid system for controlled release. Although the concepts of smart nanofibers for controlled release have been demonstrated in some studies, translation of these smart nanofibers to clinical applications could take a long way to go. Future efforts may be devoted to the development of smart electrospun nanofibers that are responsive to multiple stimuli under normal physiological conditions. However, these newly synthetic polymers could be toxic. More work needs to be done on the testing the cytotoxicity of smart nanofibers, in particular, for the newly synthesized polymers to ensure that they are at least biocompatible.

Acknowledgments

This work was supported partially from startup funds from University of Nebraska Medical Center and National Institute of General Medical Science (NIGMS) grant 2P20 GM103480-06.

References

1. Huang Z-M, Zhang Y-Z, Kotaki M, Ramakrishna S. A review on polymer nanofibers by electrospinning and their applications in nanocomposites. Compos Sci Technol. 2003; 63(15):2223–53.
2. Liu Z, Sun DD, Guo P, Leckie JO. An efficient bicomponent TiO2/SnO2 nanofiber photocatalyst fabricated by electrospinning with a side-by-side dual spinneret method. Nano Lett. 2007; 7(4): 1081–85. [PubMed: 17425281]
3. Li D, Xia Y. Direct fabrication of composite and ceramic hollow nanofibers by electrospinning. Nano Lett. 2004; 4(5):933–38.
4. Li D, Xia Y. Fabrication of titania nanofibers by electrospinning. Nano Lett. 2003; 3(4):555–60.
5. McCann JT, Li D, Xia Y. Electrospinning of nanofibers with core-sheath, hollow, or porous structures. J Mater Chem. 2005; 15(7):735–38.
6. Huang C, Soenen SJ, Rejman J, et al. Stimuli-responsive electrospun fibers and their applications. Chem Soc Rev. 2011; 40(5):2417–34. [PubMed: 21390366]
7. De Magnete, Gilbert W. Magneticisque Corporibus, et de Magno Magnete Tellure. London: Peter Short; p. 1628
8. Boys CV. On the production, properties, and some suggested uses of the finest threads. Proc Phys Soc Lond. 1887; 9(1):8.

9. Cooley, JF. Improved methods of and apparatus for electrically separating the relatively volatile liquid component from the component of relatively fixed substances of composite fluids. United Kingdom patent application GB 06385. 1900 May.
10. Doshi, Jayesh, Reneker, Darrell H. Electrospinning process and applications of electrospun fibers. Industry Applications Society Annual Meeting; 1993; Conference Record of the 1993 IEEE: IEEE; 1993.
11. Reneker DH, Chun I. Nanometre diameter fibres of polymer, produced by electrospinning. Nanotechnology. 1996; 7(3):216–23.
12. Reneker DH, Yarin AL, Fong H, Koombhongse S. Bending instability of electrically charged liquid jets of polymer solutions in electrospinning. J Appl Phys. 2000; 87(9):4531–47.
13. Hohman MM, Shin M, Rutledge G, Brenner MP. Electrospinning and electrically forced jets. I. stability theory. Phys Fluids 1994-Present. 2001; 13(8):2201–20.
14. Shin YM, Hohman MM, Brenner MP, Rutledge GC. Experimental characterization of electrospinning: the electrically forced jet and instabilities. Polymer. 2001; 42(25):09955–67.
15. Taylor G. Disintegration of water drops in an electric field. Proc Roy Soc Lond Ser Math Phys Sci. 1964; 280(1382):383–97.
16. Zhang C, Yuan X, Wu L, Han Y, Sheng J. Study on morphology of electrospun poly(vinyl alcohol) mats. Eur Polym J. 2005; 41(3):423–32.
17. Zong X, Kim K, Fang D, Ran S, Hsiao BS, Chu B. Structure and process relationship of electrospun bioabsorbable nanofiber membranes. Polymer. 2002; 43(16):4403–12.
18. Acharya M, Arumugam GK, Heiden PA. Dual electric field induced alignment of electrospun nanofibers. Macromol Mater Eng. 2008; 293(8):666–74.
19. Deitzel JM, Kleinmeyer J, Harris D, Beck Tan NC. The effect of processing variables on the morphology of electrospun nanofibers and textiles. Polymer. 2001; 42(1):261–72.
20. Hayati I, Bailey AI, Tadros TF. Investigations into the mechanisms of electrohydrodynamic spraying of liquids: I. effect of electric field and the environment on pendant drops and factors affecting the formation of stable jets and atomization. J Colloid Interface Sci. 1987; 117(1):205–21.
21. Cai S, Xu H, Jiang Q, Yang Y. Novel 3D electrospun scaffolds with fibers oriented randomly and evenly in three dimensions to closely mimic the unique architectures of extracellular matrices in soft tissues: fabrication and mechanism study. Langmuir. 2013; 29(7):2311–18. [PubMed: 23390966]
22. Huang S-H, Chien T-C, Hung K-Y. Selective deposition of electrospun alginate-based nanofibers onto cell-repelling hydrogel surfaces for cell-based microarrays. Curr Nanosci. 2011; 7(2):267–74.
23. Li D, Wang Y, Xia Y. Electrospinning of polymeric and ceramic nanofibers as uniaxially aligned arrays. Nano Lett. 2003; 3(8):1167–71.
24. Matthews JA, Wnek GE, Simpson DG, Bowlin GL. Electrospinning of collagen nanofibers. Biomacromolecules. 2002; 3(2):232–38. [PubMed: 11888306]
25. Xie J, MacEwan MR, Ray WZ, Liu W, Siewe DY, Xia Y. Radially aligned, electrospun nanofibers as dural substitutes for wound closure and tissue regeneration applications. ACS Nano. 2010; 4(9): 5027–36. [PubMed: 20695478]
26. Yang D, Lu B, Zhao Y, Jiang X. Fabrication of aligned fibrous arrays by magnetic electrospinning. Adv Mater. 2007; 19(21):3702–6.
27. Liu Y, Zhang X, Xia Y, Yang H. Magnetic-field-assisted electrospinning of aligned straight and wavy polymeric nanofibers. Adv Mater. 2010; 22(22):2454–57. [PubMed: 20376855]
28. Megelski S, Stephens JS, Chase DB, Rabolt JF. Micro- and nanostructured surface morphology on electrospun polymer fibers. Macromolecules. 2002; 35(22):8456–66.
29. Tripatanasuwan S, Zhong Z, Reneker DH. Effect of evaporation and solidification of the charged jet in electrospinning of poly(ethylene oxide) aqueous solution. Polymer. 2007; 48(19):5742–46.
30. Xin X, Hussain M, Mao JJ. Continuing differentiation of human mesenchymal stem cells and induced chondrogenic and osteogenic lineages in electrospun PLGA nanofiber scaffold. Biomaterials. 2007; 28(2):316–25. [PubMed: 17010425]
31. Langer R, Vacanti JP. Tissue engineering. Science. 1993; 260(5110):20–26. [PubMed: 17793517]

32. Boland ED, Wnek GE, Simpson DG, Pawlowski KJ, Bowlin GL. Tailoring tissue engineering scaffolds using electrostatic processing techniques: a study of poly(glycolic acid) electrospinning. J Macromol Sci Part A. 2001; 38(12):1231–43.
33. Li W-J, Laurencin CT, Caterson EJ, Tuan RS, Ko FK. Electrospun nanofibrous structure: a novel scaffold for tissue engineering. J Biomed Mater Res. 2002; 60(4):613–21. [PubMed: 11948520]
34. Yoshimoto H, Shin YM, Terai H, Vacanti JP. A biodegradable nanofiber scaffold by electrospinning and its potential for bone tissue engineering. Biomaterials. 2003; 24(12):2077–82. [PubMed: 12628828]
35. Mo XM, Xu CY, Kotaki M, Ramakrishna S. Electrospun P(LLA-CL) nanofiber: a biomimetic extracellular matrix for smooth muscle cell and endothelial cell proliferation. Biomaterials. 2004; 25(10):1883–90. [PubMed: 14738852]
36. Yang F, Murugan R, Wang S, Ramakrishna S. Electrospinning of nano/micro scale poly(L-lactic acid) aligned fibers and their potential in neural tissue engineering. Biomaterials. 2005; 26(15): 2603–10. [PubMed: 15585263]
37. Min B-M, Lee G, Kim SH, Nam YS, Lee TS, Park WH. Electrospinning of silk fibroin nanofibers and its effect on the adhesion and spreading of normal human keratinocytes and fibroblasts in vitro. Biomaterials. 2004; 25(7–8):1289–97. [PubMed: 14643603]
38. Li M, Mondrinos MJ, Gandhi MR, Ko FK, Weiss AS, Lelkes PI. Electrospun protein fibers as matrices for tissue engineering. Biomaterials. 2005; 26(30):5999–6008. [PubMed: 15894371]
39. Huang Y, Onyeri S, Siewe M, Moshfeghian A, Madihally SV. In vitro characterization of chitosan–gelatin scaffolds for tissue engineering. Biomaterials. 2005; 26(36):7616–27. [PubMed: 16005510]
40. Sun Z, Zussman E, Yarin Al, Wendorff Jh, Greiner A. Compound core–shell polymer nanofibers by co-electrospinning. Adv Mater. 2003; 15(22):1929–32.
41. Qi, Hu P, Xu J, Wang. Encapsulation of drug reservoirs in fibers by emulsion electrospinning: morphology characterization and preliminary release assessment. Biomacromolecules. 2006; 7(8): 2327–30. [PubMed: 16903678]
42. Yoo HS, Kim TG, Park TG. Surface-functionalized electrospun nanofibers for tissue engineering and drug delivery. Adv Drug Deliv Rev. 2009; 61(12):1033–42. [PubMed: 19643152]
43. Badami AS, Kreke MR, Thompson MS, Riffle JS, Goldstein AS. Effect of fiber diameter on spreading, proliferation, and differentiation of osteoblastic cells on electrospun poly(lactic acid) substrates. Biomaterials. 2006; 27(4):596–606. [PubMed: 16023716]
44. Chew SY, Mi R, Hoke A, Leong KW. The effect of the alignment of electrospun fibrous scaffolds on schwann cell maturation. Biomaterials. 2008; 29(6):653–61. [PubMed: 17983651]
45. Christopherson GT, Song H, Mao H-Q. The influence of fiber diameter of electrospun substrates on neural stem cell differentiation and proliferation. Biomaterials. 2009; 30(4):556–64. [PubMed: 18977025]
46. Li W-J, Tuli R, Okafor C, Derfoul A, Danielson KG, et al. A three-dimensional nanofibrous scaffold for cartilage tissue engineering using human mesenchymal stem cells. Biomaterials. 2005; 26(6):599–609. [PubMed: 15282138]
47. Li C, Vepari C, Jin H-J, Kim HJ, Kaplan DL. Electrospun silk-BMP-2 scaffolds for bone tissue engineering. Biomaterials. 2006; 27(16):3115–24. [PubMed: 16458961]
48. Sahoo S, Ang LT, Goh JC-H, Toh S-L. Growth factor delivery through electrospun nanofibers in scaffolds for tissue engineering applications. J Biomed Mater Res A. 2010; 93A(4):1539–50.
49. Khil M-S, Cha D-I, Kim H-Y, Kim I-S, Bhattarai N. Electrospun nanofibrous polyurethane membrane as wound dressing. J Biomed Mater Res B Appl Biomater. 2003; 67B(2):675–79.
50. Zhou Y, Yang D, Chen X, Xu Q, Lu F, Nie J. Electrospun water-soluble carboxyethyl chitosan/poly(vinyl alcohol) nanofibrous membrane as potential wound dressing for skin regeneration. Biomacromolecules. 2008; 9(1):349–54. [PubMed: 18067266]
51. Jayakumar R, Prabaharan M, Sudheesh Kumar PT, Nair SV, Tamura H. Biomaterials based on chitin and chitosan in wound dressing applications. Biotechnol Adv. 2011; 29(3):322–37. [PubMed: 21262336]
52. Ignatova M, Manolova N, Markova N, Rashkov I. Electrospun non-woven nanofibrous hybrid mats based on chitosan and PLA for wound-dressing applications. Macromol Biosci. 2009; 9(1):102–11. [PubMed: 18855947]

53. Rujitanaroj P, Pimpha N, Supaphol P. Wound-dressing materials with antibacterial activity from electrospun gelatin fiber mats containing silver nanoparticles. Polymer. 2008; 49(21):4723–32.
54. Ignatova M, Manolova N, Rashkov I. Electrospinning of poly(vinyl pyrrolidone)–iodine complex and poly(ethylene oxide)/poly(vinyl pyrrolidone)–iodine complex – a prospective route to antimicrobial wound dressing materials. Eur Polym J. 2007; 43(5):1609–23.
55. Thakur RA, Florek CA, Kohn J, Michniak BB. Electrospun nanofibrous polymeric scaffold with targeted drug release profiles for potential application as wound dressing. Int J Pharm. 2008; 364(1):87–93. [PubMed: 18771719]
56. Choi JS, Leong KW, Yoo HS. In vivo wound healing of diabetic ulcers using electrospun nanofibers immobilized with human epidermal growth factor (EGF). Biomaterials. 2008; 29(5): 587–96. [PubMed: 17997153]
57. Sheng X, Fan L, He C, Zhang K, Mo X, Wang H. Vitamin e-loaded silk fibroin nanofibrous mats fabricated by green process for skin care application. Int J Biol Macromol. 2013; 56:49–56. [PubMed: 23396066]
58. Sheikh FA, Kanjwal MA, Saran S, Chung W-J, Kim H. Polyurethane nanofibers containing copper nanoparticles as future materials. Appl Surf Sci. 2011; 257(7):3020–26.
59. Ding B, Kim J, Miyazaki Y, Shiratori S. Electrospun nanofibrous membranes coated quartz crystal microbalance as gas sensor for NH3 detection. Sens Actuators B-Chem. 2004; 101(3):373–80.
60. Kim I-D, Rothschild A, Lee BH, Kim DY, Jo SM, Tuller HL. Ultrasensitive chemiresistors based on electrospun TiO2 nanofibers. Nano Lett. 2006; 6(9):2009–13. [PubMed: 16968017]
61. Choi S-W, Park JY, Kim SS. Synthesis of SnO2–ZnO core–shell nanofibers via a novel two-step process and their gas sensing properties. Nanotechnology. 2009; 20(46):465603. [PubMed: 19847030]
62. Lim SK, Hwang S-H, Chang D, Kim S. Preparation of mesoporous In2O3 nanofibers by electrospinning and their application as a CO gas sensor. Sens Actuators B-Chem. 2010; 149(1): 28–33.
63. Wang M, Meng G, Huang Q, Qian Y. Electrospun 1,4-DHAQ-doped cellulose nanofiber films for reusable fluorescence detection of trace Cu2+ and further for Cr3+ Environ Sci Technol. 2012; 46(1):367–73. [PubMed: 22129160]
64. Sun M, Ding B, Yu J. Sensitive metal ion sensors based on fibrous polystyrene membranes modified by polyethyleneimine. RSC Adv. 2012; 2(4):1373–78.
65. Wang X, Kim Y-G, Drew C, Ku B-C, Kumar J, Samuelson LA. Electrostatic assembly of conjugated polymer thin layers on electrospun nanofibrous membranes for biosensors. Nano Lett. 2004; 4(2):331–34.
66. Sawicka K, Gouma P, Simon S. Electrospun biocomposite nanofibers for urea biosensing. Sens Actuators B-Chem. 2005; 108(1–2):585–88.
67. Wang W, Zhang L, Tong S, Li X, Song W. Three-dimensional network films of electrospun copper oxide nanofibers for glucose determination. Biosens Bioelectron. 2009; 25(4):708–14. [PubMed: 19733046]
68. Zhang N, Deng Y, Tai Q, et al. Electrospun TiO2 nanofiber-based cell capture assay for detecting circulating tumor cells from colorectal and gastric cancer patients. Adv Mater. 2012; 24(20):2756–60. [PubMed: 22528884]
69. Hou S, Zhao L, Shen Q, et al. Polymer nanofiber-embedded microchips for detection, isolation, and molecular analysis of single circulating melanoma cells. Angew Chem Int Ed. 2013; 52(12): 3379–83.
70. Zhao L, Lu Y-T, Li F, et al. High-purity prostate circulating tumor cell isolation by a polymer nanofiber-embedded microchip for whole exome sequencing. Adv Mater. 2013; 25(21):2897–2902. [PubMed: 23529932]
71. Kenawy E-R, Bowlin GL, Mansfield K, et al. Release of tetracycline hydrochloride from electrospun poly(ethylene-co-vinylacetate), poly(lactic acid), and a blend. J Control Release. 2002; 81(1–2):57–64. [PubMed: 11992678]
72. Zeng J, Xu X, Chen X, et al. Biodegradable electrospun fibers for drug delivery. J Control Release. 2003; 92(3):227–31. [PubMed: 14568403]

73. Kim K, Luu YK, Chang C, et al. Incorporation and controlled release of a hydrophilic antibiotic using poly(lactide-co-glycolide)-based electrospun nanofibrous scaffolds. J Control Release. 2004; 98(1):47–56. [PubMed: 15245888]
74. Zeng J, Aigner A, Czubayko F, Kissel T, Wendorff JH, Greiner A. Poly(vinyl alcohol) nanofibers by electrospinning as a protein delivery system and the retardation of enzyme release by additional polymer coatings. Biomacromolecules. 2005; 6(3):1484–88. [PubMed: 15877368]
75. Xie J, Wang C-H. Electrospun micro- and nanofibers for sustained delivery of paclitaxel to treat C6 glioma in vitro. Pharm Res. 2006; 23(8):1817–26. [PubMed: 16841195]
76. Mano JF. Stimuli-responsive polymeric systems for biomedical applications. Adv Eng Mater. 2008; 10(6):515–27.
77. Mura S, Nicolas J, Couvreur P. Stimuli-responsive nanocarriers for drug delivery. Nat Mater. 2013; 12(11):991–1003. [PubMed: 24150417]
78. Alvarez-Lorenzo C, Concheiro A. Smart drug delivery systems: from fundamentals to the clinic. Chem Commun. 2014; 50(58):7743–65.
79. Mindell JA. Lysosomal acidification mechanisms. Annu Rev Physiol. 2012; 74(1):69–86. [PubMed: 22335796]
80. Boron, WF., Boulpaep, EL. Medical physiology: a cellular and molecular approach. 2nd. Philadelphia: Saunders Elsevier; 2004.
81. Grinstein S, Swallow CJ, Rotstein OD. Regulation of cytoplasmic pH in phagocytic cell function and dysfunction. Clin Biochem. 1991; 24(3):241–47. [PubMed: 1651820]
82. Kraus M, Wolf B. Implications of acidic tumor microenvironment for neoplastic growth and cancer treatment: a computer analysis. Tumour Biol. 1996; 17(3):133–54. [PubMed: 8638088]
83. Miyazaki T, Zipes DP. Presynaptic modulation of efferent sympathetic and vagal neurotransmission in the canine heart by hypoxia, high K+, low pH, and adenosine possible relevance to ischemia-induced denervation. Circ Res. 1990; 66(2):289–301. [PubMed: 2153468]
84. Schneider LA, Korber A, Grabbe S, Dissemond J. Influence of pH on wound-healing: a new perspective for wound-therapy? Arch Dermatol Res. 2007; 298(9):413–20. [PubMed: 17091276]
85. Risbud MV, Hardikar AA, Bhat SV, Bhonde RR. PH-sensitive freeze-dried chitosan–polyvinyl pyrrolidone hydrogels as controlled release system for antibiotic delivery. J Control Release. 2000; 68(1):23–30. [PubMed: 10884576]
86. Chen S-C, Wu Y-C, Mi F-L, Lin Y-H, Yu L-C, Sung H-W. A novel pH-sensitive hydrogel composed of N,O-carboxymethyl chitosan and alginate cross-linked by genipin for protein drug delivery. J Control Release. 2004; 96(2):285–300. [PubMed: 15081219]
87. Shome A, Debnath S, Das PK. Head group modulated pH-responsive hydrogel of amino acid-based amphiphiles: entrapment and release of cytochrome c and vitamin B12. Langmuir. 2008; 24(8):4280–88. [PubMed: 18324868]
88. Cao S, Hu B, Liu H. Synthesis of pH-responsive crosslinked poly[styrene-co-(maleic sodium anhydride)] and cellulose composite hydrogel nanofibers by electrospinning. Polym Int. 2009; 58(5):545–51.
89. Qi M, Li X, Yang Y, Zhou S. Electrospun fibers of acid-labile biodegradable polymers containing ortho ester groups for controlled release of paracetamol. Eur J Pharm Biopharm. 2008; 70(2):445–52. [PubMed: 18603416]
90. Cui W, Qi M, Li X, Huang S, Zhou S, Weng J. Electrospun fibers of acid-labile biodegradable polymers with acetal groups as potential drug carriers. Int J Pharm. 2008; 361(1–2):47–55. [PubMed: 18571349]
91. Yuan Z, Zhao J, Zhu W, Yang Z, Li B, et al. Ibuprofen-loaded electrospun fibrous scaffold doped with sodium bicarbonate for responsively inhibiting inflammation and promoting muscle wound healing in vivo. Biomater Sci. 2014; 2(4):502–11.
92. Fujihara K, Kotaki M, Ramakrishna S. Guided bone regeneration membrane made of polycaprolactone/calcium carbonate composite nano-fibers. Biomaterials. 2005; 26(19):4139–47. [PubMed: 15664641]
93. Oyane A, Uchida M, Yokoyama Y, Choong C, Triffitt J, Ito A. Simple surface modification of poly(ε-caprolactone) to induce its apatite-forming ability. J Biomed Mater Res A. 2005; 75A(1): 138–45.

94. Yang F, Wolke JGC, Jansen JA. Biomimetic calcium phosphate coating on electrospun poly(ε-caprolactone) scaffolds for bone tissue engineering. Chem Eng J. 2008; 137(1):154–61.

95. Jiang J, Xie J, Ma B, Bartlett DE, Xu A, Wang C-H. Mussel-inspired protein-mediated surface functionalization of electrospun nanofibers for pH-responsive drug delivery. Acta Biomater. 2014; 10(3):1324–32. [PubMed: 24287161]

96. Dinarello CA. Review: infection, fever, and exogenous and endogenous pyrogens: some concepts have changed. J Endotoxin Res. 2004; 10(4):201–22. [PubMed: 15373964]

97. Becker GJ, Waldburger M, Hughes GR, Pepys MB. Value of serum C-reactive protein measurement in the investigation of fever in systemic lupus erythematosus. Ann Rheum Dis. 1980; 39(1):50–52. [PubMed: 7377859]

98. Santolaya ME, Alvarez AM, Becker A, Cofré J, Enríquez N, et al. Prospective, multicenter evaluation of risk factors associated with invasive bacterial infection in children with cancer, neutropenia, and fever. J Clin Oncol. 2001; 19(14):3415–21. [PubMed: 11454890]

99. Crile G, Rumsey EW. Subacute thyroiditis. J Am Med Assoc. 1950; 142(7):458–62. [PubMed: 15409440]

100. Taylor LD, Cerankowski LD. Preparation of films exhibiting a balanced temperature dependence to permeation by aqueous solutions—a study of lower consolute behavior. J Polym Sci Polym Chem Ed. 1975; 13(11):2551–70.

101. Heskins M, Guillet JE. Solution properties of poly(n-isopropylacrylamide). J Macromol Sci Part-Chem. 1968; 2(8):1441–55.

102. Schild HG. Poly(n-isopropylacrylamide): experiment, theory and application. Prog Polym Sci. 1992; 17(2):163–249.

103. Fujishige S, Kubota K, Ando I. Phase transition of aqueous solutions of poly(n-isopropylacrylamide) and poly(n-isopropylmethacrylamide). J Phys Chem. 1989; 93(8):3311–13.

104. Kuramoto N, Shishido Y. Property of thermo-sensitive and redox-active poly(n-cyclopropylacrylamide-co-vinylferrocene) and poly(n-isopropylacrylamide-co-vinylferrocene). Polymer. 1998; 39(3):669–73.

105. Idziak I, Avoce D, Lessard D, Gravel D, Zhu XX. Thermosensitivity of aqueous solutions of poly(n,n-diethylacrylamide). Macromolecules. 1999; 32(4):1260–63.

106. Huang X-N, Du F-S, Zhang B, Zhao J-Y, Li Z-C. Acid-labile, thermoresponsive (meth)acrylamide polymers with pendant cyclic acetal moieties. J Polym Sci A Polym Chem. 2008; 46(13):4332–43.

107. Kirsh, YE. Water Soluble Poly-N-Vinylamides: Synthesis and Physicochemical Properties. Hoboken: John Wiley & Sons; 1998.

108. Schäfer-Soenen H, Moerkerke R, Berghmans H, Koningsveld R, Dušek K, Šolc K. Zero and off-zero critical concentrations in systems containing polydisperse polymers with very high molar masses. 2. the system water–poly(vinyl methyl ether). Macromolecules. 1997; 30(3):410–16.

109. Alexandridis P, Holzwarth JF, Hatton TA. Micellization of poly(ethylene oxide)-poly(propylene oxide)-poly(ethylene oxide) triblock copolymers in aqueous solutions: thermodynamics of copolymer association. Macromolecules. 1994; 27(9):2414–25.

110. Rockwood DN, Chase DB, Akins RE Jr, Rabolt JF. Characterization of electrospun poly(n-isopropyl acrylamide) fibers. Polymer. 2008; 49(18):4025–32.

111. Okuzaki H, Kobayashi K, Yan H. Thermo-responsive nanofiber mats. Macromolecules. 2009; 42(16):5916–18.

112. Kim Y-J, Ebara M, Aoyagi T. Temperature-responsive electrospun nanofibers for “on–off” switchable release of dextran. Sci Technol Adv Mater. 2012; 13(6):064203. [PubMed: 27877530]

113. Krishnan S, Klein A, El-Aasser MS, Sudol ED. Influence of chain transfer agent on the cross-linking of poly(n-butyl methacrylate-co-n-methylol acrylamide) latex particles and films. Macromolecules. 2003; 36(10):3511–18.

114. Huffman AS, Afrassiabi A, Dong LC. Thermally reversible hydrogels: II. delivery and selective removal of substances from aqueous solutions. J Control Release. 1986; 4(3):213–22.

115. Wang N, Zhao Y, Jiang L. Low-cost, thermoresponsive wettability of surfaces: poly(n-isopropylacrylamide)/polystyrene composite films prepared by electrospinning. Macromol Rapid Commun. 2008; 29(6):485–89.

116. Muthiah P, Hoppe SM, Boyle TJ, Sigmund W. Thermally tunable surface wettability of electrospun fiber mats: polystyrene/poly(n-isopropylacrylamide) blended versus crosslinked poly[(n-isopropylacrylamide)-co-(methacrylic acid)]. Macromol Rapid Commun. 2011; 32(21): 1716–21. [PubMed: 21994211]

117. Muthiah P, Boyle TJ, Sigmund W. Thermally induced, rapid wettability switching of electrospun blended polystyrene/poly(n-isopropylacrylamide) nanofiber mats. Macromol Mater Eng. 2013; 298(12):1251–58.

118. Chen M, Dong M, Havelund R, et al. Thermo-responsive core–sheath electrospun nanofibers from poly (n-isopropylacrylamide)/polycaprolactone blends. Chem Mater. 2010; 22(14):4214–21.

119. Lin X, Tang D, Gu S, Du H, Jiang E. Electrospun poly(n-isopropylacrylamide)/poly(caprolactone)-based polyurethane nanofibers as drug carriers and temperature-controlled release. New J Chem. 2013; 37(8):2433–39.

120. Lin X, Tang D, Cui W, Cheng Y. Controllable drug release of electrospun thermoresponsive poly(n-isopropylacrylamide)/poly(2-acrylamido-2- methylpropanesulfonic acid) nanofibers. J Biomed Mater Res A. 2012; 100A(7):1839–45.

121. Song F, Wang X-L, Wang Y-Z. Poly (n-isopropylacrylamide)/poly (ethylene oxide) blend nanofibrous scaffolds: thermo-responsive carrier for controlled drug release. Colloids Surf B Biointerfaces. 2011; 88(2):749–54. [PubMed: 21889883]

122. Jeong SI, Lee YM, Lee J, Shin YM, Shin H, et al. Preparation and characterization of temperature-sensitive poly(n-isopropylacrylamide)-g-poly(l-lactide-co-ε-caprolactone) nanofibers. Macromol Res. 2008; 16(2):139–48.

123. Coldiron BM. Thinning of the ozone layer: facts and consequences. J Am Acad Dermatol. 1992; 27(5, Part 1):653–62. [PubMed: 1430383]

124. Guiriec P, Hapiot P, Moiroux J, Neudeck A, Pinson J, Tavani C. Isomerization of azo compounds. Cleavage recombination mechanism of azosulfides. J Phys Chem A. 1999; 103(28):5490–5500.

125. Yagai S, Kitamura A. Recent advances in photoresponsive supramolecular self-assemblies. Chem Soc Rev. 2008; 37(8):1520–29. [PubMed: 18648678]

126. Feringa, BL., Browne, Wesley R., editors. Molecular Switches. 2nd. John Wiley & Sons; 2011.

127. Browne WR, Feringa BL. Making molecular machines work. Nat Nanotechnol. 2006; 1(1):25–35. [PubMed: 18654138]

128. Andréasson J, Pischel U, Straight SD, Moore TA, Moore AL, Gust D. All-photonic multifunctional molecular logic device. J Am Chem Soc. 2011; 133(30):11641–48. [PubMed: 21563823]

129. Sousa FBD, Guerreiro JDT, Ma M, Anderson DG, Drum CL, et al. Photo-response behavior of electrospun nanofibers based on spiropyran-cyclodextrin modified polymer. J Mater Chem. 2010; 20(44):9910–17. [PubMed: 28210069]

130. Chen M, Besenbacher F. Light-driven wettability changes on a photoresponsive electrospun mat. ACS Nano. 2011; 5(2):1549–55. [PubMed: 21288000]

131. Fu G-D, Xu L-Q, Yao F, Li G-L, Kang E-T. Smart nanofibers with a photoresponsive surface for controlled release. ACS Appl Mater Interfaces. 2009; 1(11):2424–27. [PubMed: 20356110]

132. Rekharsky MV, Inoue Y. Complexation Thermodynamics of Cyclodextrins. Chem Rev. 1998; 98(5):1875–918. [PubMed: 11848952]

133. Quan C-Y, Chen J-X, Wang H-Y, et al. Core–shell nanosized assemblies mediated by the α–β cyclodextrin dimer with a tumor-triggered targeting property. ACS Nano. 2010; 4(7):4211–19. [PubMed: 20521828]

134. Danil de Namor AF, Traboulssi R, Lewis DFV. Host properties of cyclodextrins towards anion constituents of antigenic determinants. A thermodynamic study in water and in N,N-dimethylformamide. J Am Chem Soc. 1990; 112(23):8442–47.

135. Xiao, Wang, Chen, Wei-Hai, Xu, Xiao-Ding, et al. Design of a cellular-uptake- shielding “plug and play” template for photo controllable drug release. Adv Mater. 2011; 23(31):3526–30. [PubMed: 21726005]

136. Pouget J-P, Douki T, Richard M-J, Cadet J. DNA damage induced in cells by γ and UVA radiation as measured by HPLC/GC-MS and HPLC–EC and comet assay. Chem Res Toxicol. 2000; 13(7):541–49. [PubMed: 10898585]

137. Huang X, El-Sayed IH, Qian W, El-Sayed MA. Cancer cell imaging and photothermal therapy in the near-infrared region by using gold nanorods. J Am Chem Soc. 2006; 128(6):2115–20. [PubMed: 16464114]

138. Pissuwan D, Valenzuela SM, Cortie MB. Therapeutic possibilities of plasmonically heated gold nanoparticles. Trends Biotechnol. 2006; 24(2):62–67. [PubMed: 16380179]

139. Huang X, Jain PK, El-Sayed IH, El-Sayed MA. Plasmonic photothermal therapy (PPTT) using gold nanoparticles. Lasers Med Sci. 2008; 23(3):217–28. [PubMed: 17674122]

140. Baughman RH. Conducting polymer artificial muscles. Synth Met. 1996; 78(3):339–53.

141. Tanaka T, Nishio I, Sun S-T, Ueno-Nishio S. Collapse of gels in an electric field. Science. 1982; 218(4571):467–69. [PubMed: 17808541]

142. Ramanathan S, Block LH. The use of chitosan gels as matrices for electrically-modulated drug delivery. J Control Release. 2001; 70(1–2):109–23. [PubMed: 11166412]

143. Jensen M, Birch Hansen P, Murdan S, Frokjaer S, Florence AT. Loading into and electro-stimulated release of peptides and proteins from chondroitin 4-sulphate hydrogels. Eur J Pharm Sci. 2002; 15(2):139–48. [PubMed: 11849910]

144. Smela E. Conjugated polymer actuators for biomedical applications. Adv Mater. 2003; 15(6): 481–94.

145. Palakodeti R, Kessler MR. Influence of frequency and prestrain on the mechanical efficiency of dielectric electroactive polymer actuators. Mater Lett. 2006; 60(29–30):3437–40.

146. Carpi, F.Rossi, DD.Kornbluh, R.Pelrine, RE., Sommer-Larsen, P., editors. Dielectric elastomers as electromechanical transducers: fundamentals, materials, devices, models and applications of an emerging electroactive polymer technology. Amsterdam: Elsevier; 2011.

147. Inganäs O, Lundström I. Carbon nanotube muscles. Science. 1999; 284(5418):1281–82.

148. Abidian MR, Kim D-H, Martin DC. Conducting-polymer nanotubes for controlled drug release. Adv Mater. 2006; 18(4):405–9. [PubMed: 21552389]

149. Pernaut J-M, Reynolds JR. Use of conducting electroactive polymers for drug delivery and sensing of bioactive molecules a redox chemistry approach. J Phys Chem B. 2000; 104(17): 4080–90.

150. Yun J, Im JS, Lee Y-S, Kim H-I. Electro-responsive transdermal drug delivery behavior of PVA/PAA/MWCNT nanofibers. Eur Polym J. 2011; 47(10):1893–1902.

151. Shvedova A, Castranova V, Kisin E, Schwegler-Berry D, Murray A, et al. Exposure to carbon nanotube material: assessment of nanotube cytotoxicity using human keratinocyte cells. J Toxicol Environ Health A. 2003; 66(20):1909–26. [PubMed: 14514433]

152. Schenck JF. Physical interactions of static magnetic fields with living tissues. Prog Biophys Mol Biol. 2005; 87(2–3):185–204. [PubMed: 15556658]

153. Weissleder R. A clearer vision for in vivo imaging. Nat Biotechnol. 2001; 19(4):316–17. [PubMed: 11283581]

154. Theysohn JM, Maderwald S, Kraff O, Moenninghoff C, Ladd ME, Ladd SC. Subjective acceptance of 7 tesla MRI for human imaging. Magn Reson Mater Phys Biol Med. 2008; 21(1–2):63–72.

155. Wang M, Singh H, Hatton TA, Rutledge GC. Field-responsive superparamagnetic composite nanofibers by electrospinning. Polymer. 2004; 45(16):5505–14.

156. Tan ST, Wendorff JH, Pietzonka C, Jia ZH, Wang GQ. Biocompatible and biodegradable polymer nanofibers displaying superparamagnetic properties. Chem Phys Chem. 2005; 6(8):1461–65. [PubMed: 16007710]

157. Li D, McCann JT, Xia Y. Use of electrospinning to directly fabricate hollow nanofibers with functionalized inner and outer surfaces. Small. 2005; 1(1):83–86. [PubMed: 17193354]

158. Bean CP, Livingston JD. Superparamagnetism. J Appl Phys. 1959; 30(4):S120–29.

159. Hussain SM, Hess KL, Gearhart JM, Geiss KT, Schlager JJ. In vitro toxicity of nanoparticles in BRL 3A rat liver cells. Toxicol In Vitro. 2005; 19(7):975–83. [PubMed: 16125895]

160. Ankamwar B, Lai TC, Huang JH, Liu RS, Hsiao M, et al. Biocompatibility of Fe3O4 nanoparticles evaluated by in vitro cytotoxicity assays using normal, glia and breast cancer cells. Nanotechnology. 2010; 21(7):075102.

161. Wang L, Wang M, Topham PD, Huang Y. Fabrication of magnetic drug-loaded polymeric composite nanofibres and their drug release characteristics. RSC Adv. 2012; 2(6):2433–38.

162. Savva I, Odysseos AD, Evaggelou L, Marinica O, Vasile E, et al. Fabrication, characterization, and evaluation in drug release properties of magnetoactive poly(ethylene oxide)–poly(l-lactide) electrospun membranes. Biomacromolecules. 2013; 14(12):4436–46. [PubMed: 24261831]

163. Hergt R, Hiergeist R, Hilger I, Kaiser WA, Lapatnikov Y, et al. Maghemite nanoparticles with very high AC-losses for application in RF-magnetic hyperthermia. J Magn Magn Mater. 2004; 270(3):345–57.

164. Pankhurst QA, Connolly J, Jones SK, Dobson J. Applications of magnetic nanoparticles in biomedicine. J Phys Appl Phys. 2003; 36(13):R167–81.

165. Rong, C-b, Li, D., Nandwana, V., Poudyal, N., Ding, Y., et al. Size-dependent chemical and magnetic ordering in L10-FePt nanoparticles. Adv Mater. 2006; 18(22):2984–88.

166. Chen H, Hsieh Y-L. Ultrafine hydrogel fibers with dual temperature- and pH-responsive swelling behaviors. J Polym Sci Part Polym Chem. 2004; 42(24):6331–39.

167. Li L, Hsieh Y-L. Ultra-fine polyelectrolyte hydrogel fibres from poly(acrylic acid)/poly(vinyl alcohol). Nanotechnology. 2005; 16(12):2852–60.

168. Liu H, Zhen M, Wu R. Ionic-strength- and pH-responsive poly[acrylamide-co-(maleic acid)] hydrogel nanofibers. Macromol Chem Phys. 2007; 208(8):874–80.

169. Chunder A, Sarkar S, Yu Y, Zhai L. Fabrication of ultrathin polyelectrolyte fibers and their controlled release properties. Colloids Surf B Biointerfaces. 2007; 58(2):172–79. [PubMed: 17418541]

170. Gupta P, Vermani K, Garg S. Hydrogels: from controlled release to pH-responsive drug delivery. Drug Discov Today. 2002; 7(10):569–79. [PubMed: 12047857]

171. Buwalda SJ, Boere KWM, Dijkstra PJ, Feijen J, Vermonden T, Hennink WE. Hydrogels in a historical perspective: from simple networks to smart materials. J Control Release. 2014; 190:254–73. [PubMed: 24746623]

172. Ganta S, Devalapally H, Shahiwala A, Amiji M. A review of stimuli-responsive nanocarriers for drug and gene delivery. J Control Release. 2008; 126(3):187–204. [PubMed: 18261822]

173. Elsabahy M, Wooley KL. Design of polymeric nanoparticles for biomedical delivery applications. Chem Soc Rev. 2012; 41(7):2545–61. [PubMed: 22334259]

174. Cammas S, Suzuki K, Sone C, Sakurai Y, Kataoka K, Okano T. Thermo-responsive polymer nanoparticles with a core-shell micelle structure as site-specific drug carriers. J Control Release. 1997; 48(2–3):157–64.

175. Phase 3 study of thermodox with radiofrequency ablation (RFA) in treatment of hepatocellular carcinoma (HCC) [homepage on the internet]. The U.S. National Institutes of Health; [cited 2014 Nov 13]. Available from: (www.clinicaltrials.gov)

176. Müller RH, Mäder K, Gohla S. Solid lipid nanoparticles (SLN) for controlled drug delivery – a review of the state of the art. Eur J Pharm Biopharm. 2000; 50(1):161–77. [PubMed: 10840199]

177. Panyam J, Labhasetwar V. Biodegradable nanoparticles for drug and gene delivery to cells and tissue. Adv Drug Deliv Rev. 2003; 55(3):329–47. [PubMed: 12628320]

178. Cheng Y, Xu Z, Ma M, Xu T. Dendrimers as drug carriers: applications in different routes of drug administration. J Pharm Sci. 2008; 97(1):123–43. [PubMed: 17721949]

179. Brannon-Peppas L, Blanchette JO. Nanoparticle and targeted systems for cancer therapy. Adv Drug Deliv Rev. 2012; 64:206–12.

180. Park Y-S, Cho J-Y, Lee S-J, Hwang CI. Modified titanium implant as a gateway to the human body: the implant mediated drug delivery system. BioMed Res Int. 2014:e801358.

181. Sill TJ, von Recum HA. Electrospinning: applications in drug delivery and tissue engineering. Biomaterials. 2008; 29(13):1989–2006. 2014. [PubMed: 18281090]

182. Knockenhauer, Kevin E., Sawicka, KM., Roemer, EJ., et al. Protective antigen composite nanofibers as a transdermal anthrax vaccine. Engineering in Medicine and Biology Society, 2008. EMBS 2008. 30th Annual International Conference of the IEEE. IEEE; 2008.

183. Ngawhirunpat T, Opanasopit P, Rojanarata T, Akkaramongkolporn P, Ruktanonchai U, Supaphol P. Development of meloxicam-loaded electrospun polyvinyl alcohol mats as a transdermal therapeutic agent. Pharm Dev Technol. 2008; 14(1):73–82.

184. Yu D-G, Shen X-X, Branford-White C, White K, Zhu L-M, Bligh SWA. Oral fast-dissolving drug delivery membranes prepared from electrospun polyvinylpyrrolidone ultrafine fibers. Nanotechnology. 2009; 20(5):055104. [PubMed: 19417335]

185. Huang C, Soenen SJ, van Gulck E, Vanham G, Rejman J, et al. Electrospun cellulose acetate phthalate fibers for semen induced anti-HIV vaginal drug delivery. Biomaterials. 2012; 33(3): 962–69. [PubMed: 22018388]

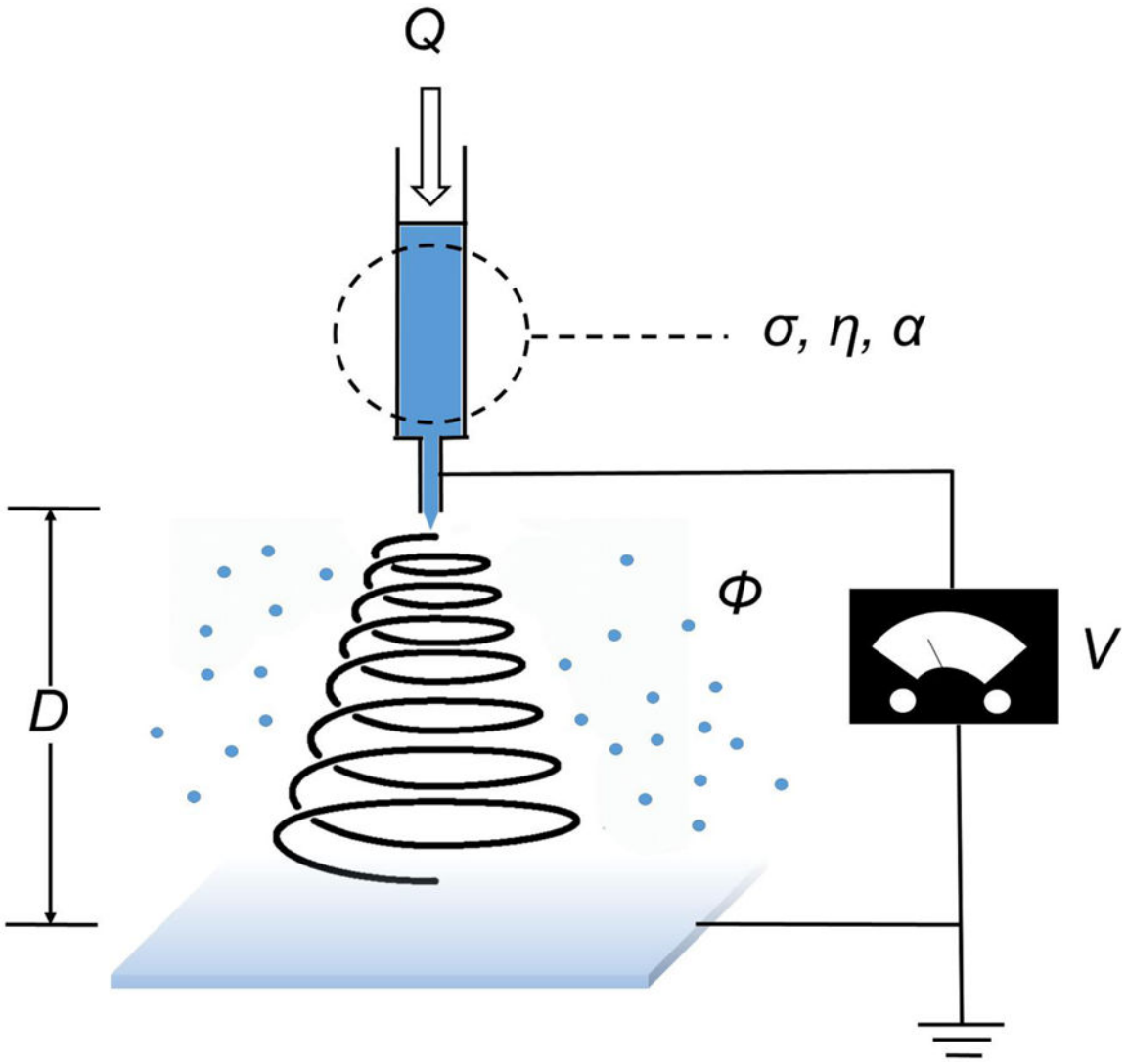

Fig. (1).
Schematic illustrating the experimental setup and primary adjustable parameters for electrospinning. Q: flow rate; V: high voltage; D: distance from nozzle to collector; σ, η, and α: conductivity, viscosity, and relative volatility of the polymer solution, respectively; ϕ: relative humidity.

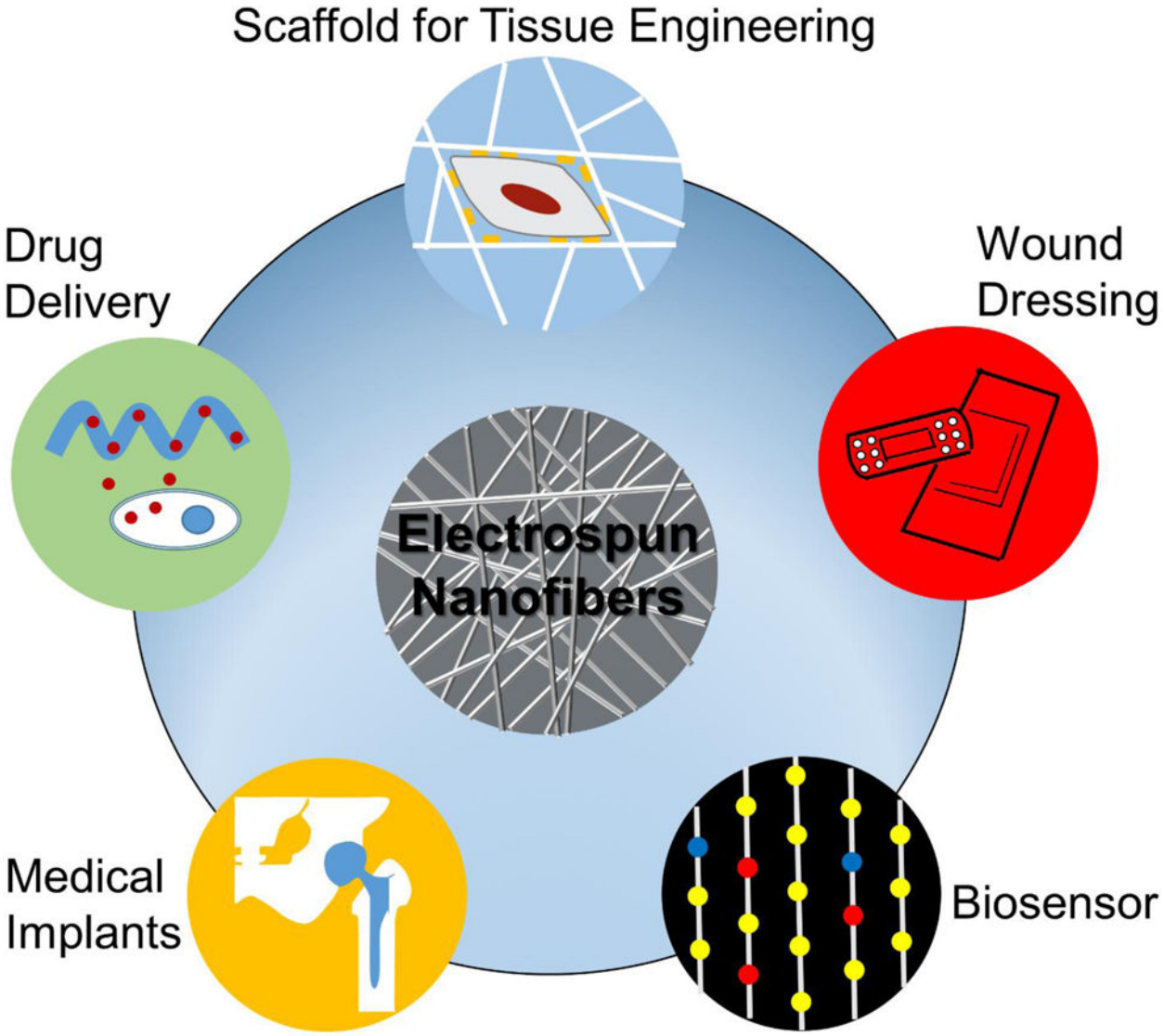

Fig. (2).
Various applications of electrospun nanofibers in biomedical research.

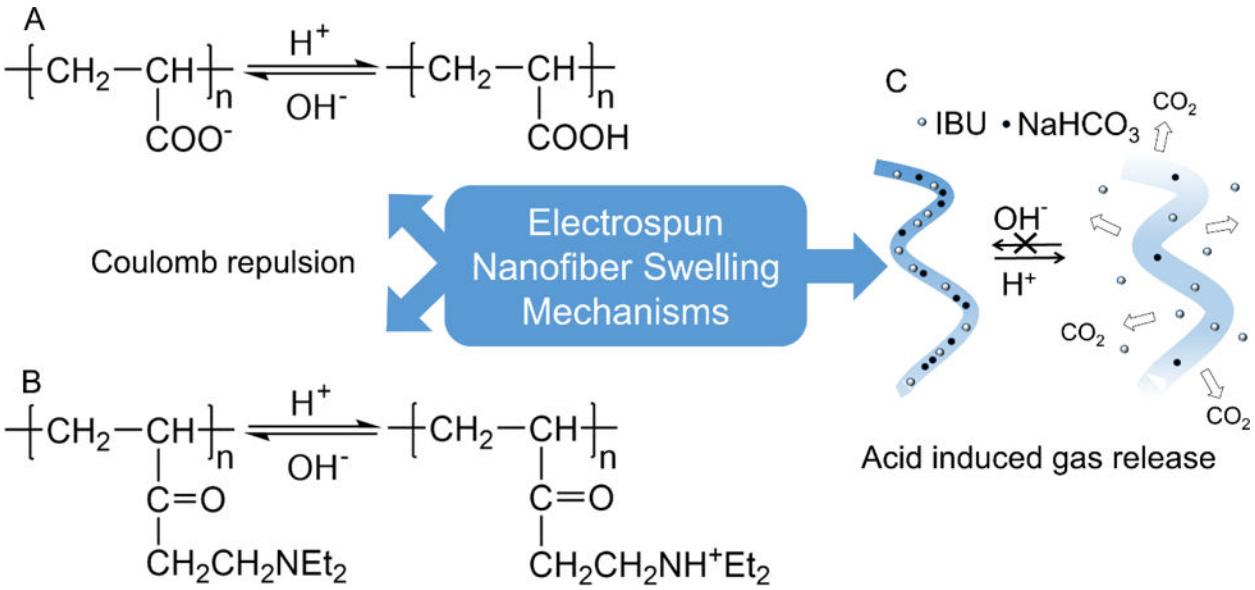

Fig. (3).

Primary swelling schemes in pH sensitive electrospun nanofibers. (A, B) Coulomb repulsion forces generated by the charged amine and carboxyl groups at different pH values. (C) Gas releasing electrospun nanofibers. (Adapted from ref. [91])

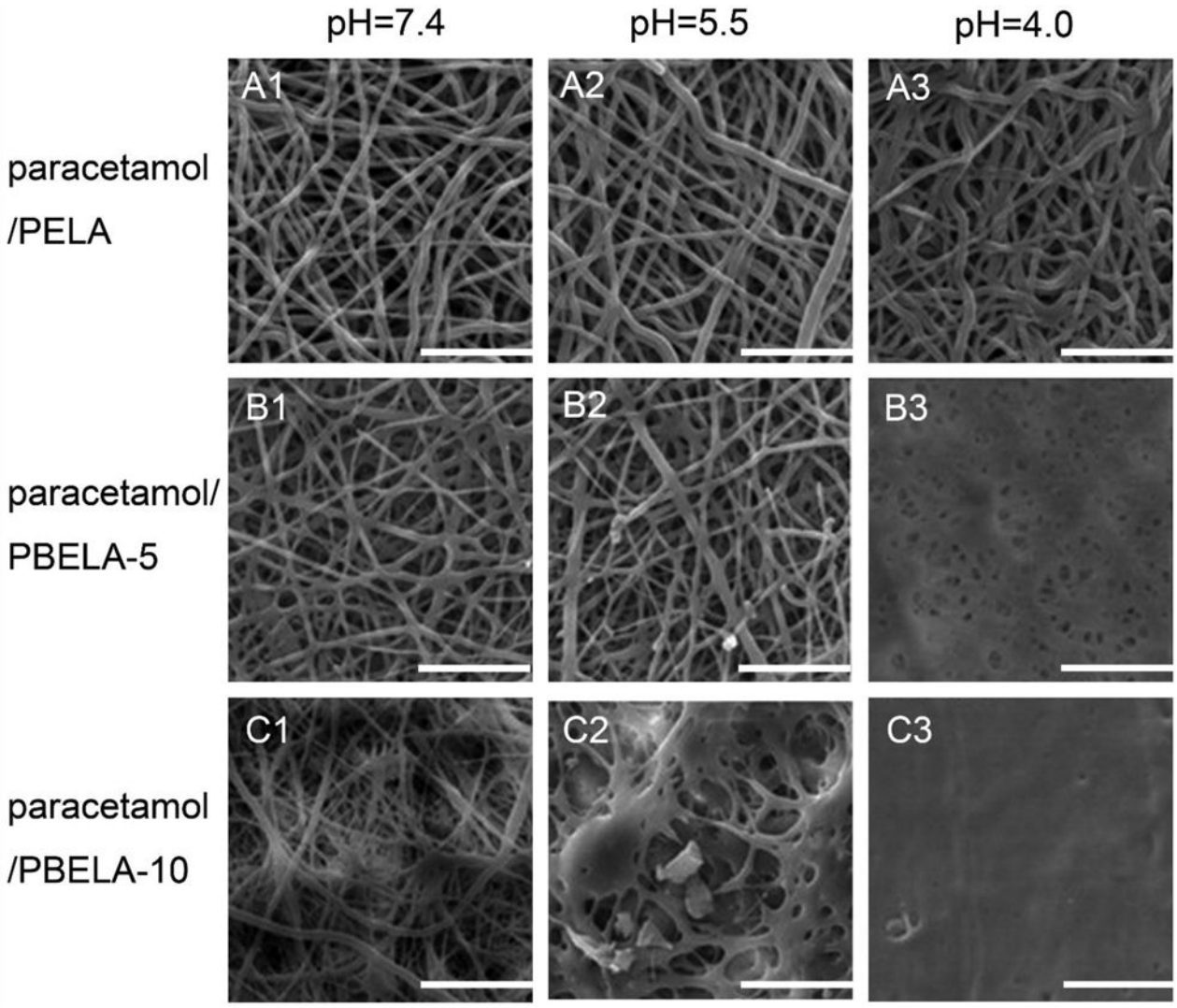

Fig. (4).

SEM images of Paracetamol loaded electrospun PLA-PEG-PLA (PELA) and copolymer PLA-PBE-PLA (PBELA) fibrous mats responding to different pH values: 7.4, 5.5, and 4.0. The scale bar is 20 μm. The number following PBELA indicates the amount of PBE in unit of wt%. (Reprinted from ref. [90])

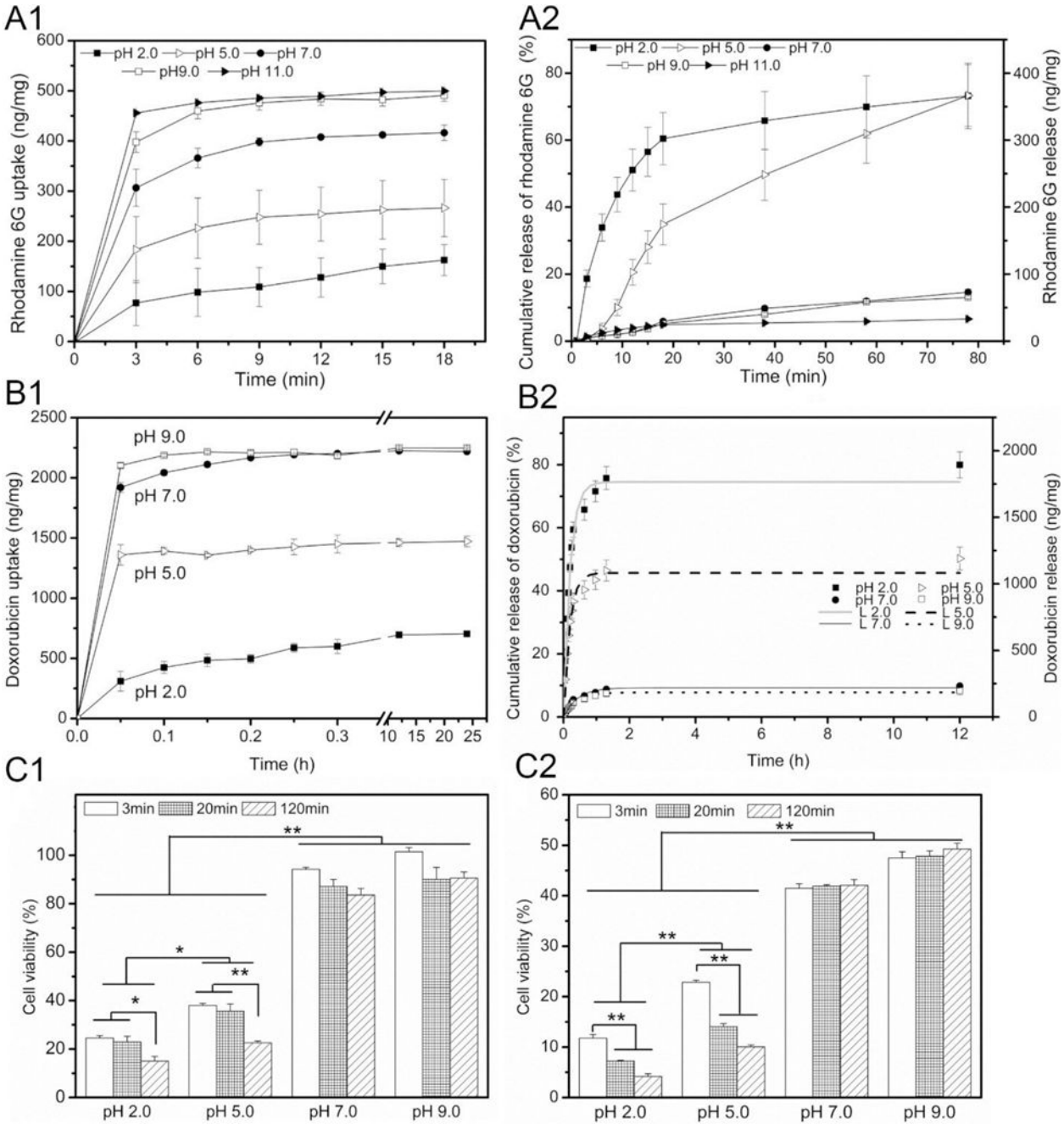

Fig. (5).

(A1) Rhodamine 6G loading kinetics and (A2) release profiles of polydopamine-coated PCL fiber samples in aqueous solutions at pH 2.0, 5.0, 7.0, 9.0 and 11.0. (B1) Doxorubicin loading kinetics and (B2) release profiles of polydopamine-coated PCL fiber samples in aqueous solutions at pH 2.0, 5.0, 7.0 and 9.0. The *in vitro* release data were fitted with a desorption model. L2.0: α = 0.74, τr = 0.24; L5.0: α = 0.46, τr = 0.22; L7.0: α = 0.09, τr = 0.51; L9.0: α = 0.08, τr = 0.47. H1299 cell viability quantified by MTT assay treated with release media for (C1) 1 day and (C2) 3 days. The released media from doxorubicin-loaded, polydopamine-coated PCL fiber samples were collected at different times (3 min, 20 min

and 120 min) from solutions with pH 2.0, 5.0, 7.0 and 9.0 (*$p < 0.05$, **$p < 0.01$). (Reprinted from ref. [95])

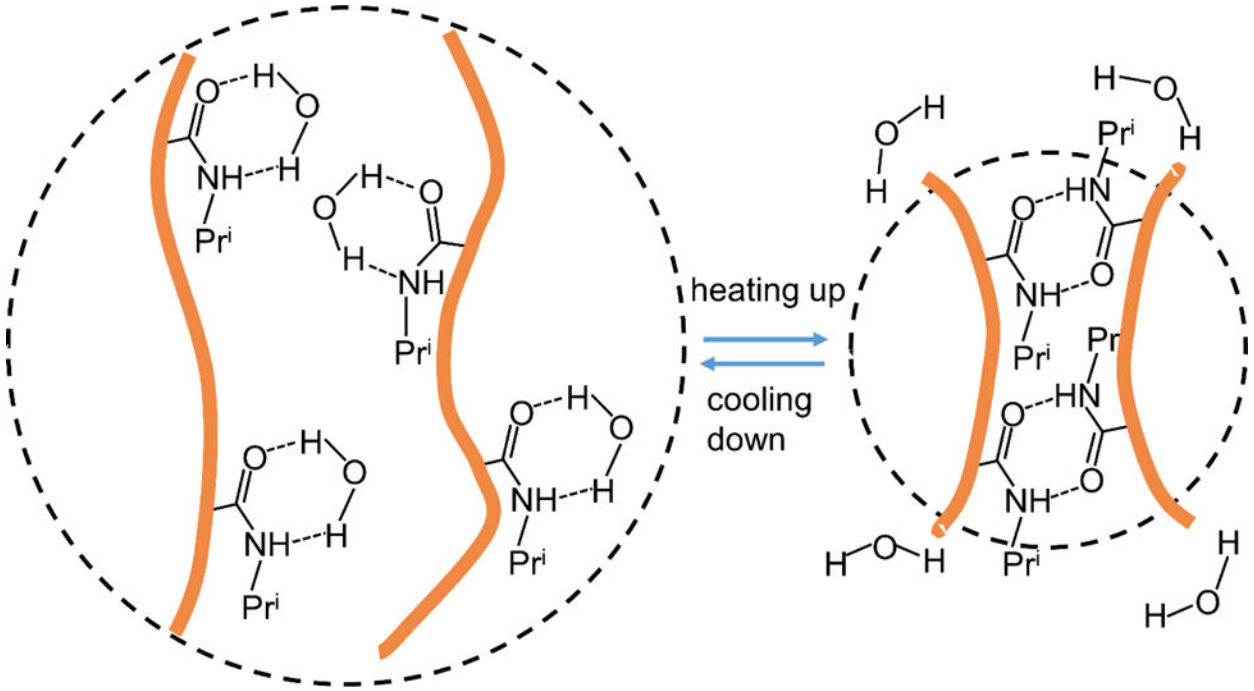

Fig. (6).

Schematic illustration of thermal response of PNIPAAM polymers and mechanism of the change of polymer volume due to reformations of hydrogen bonds. (Adapted from ref. [118])

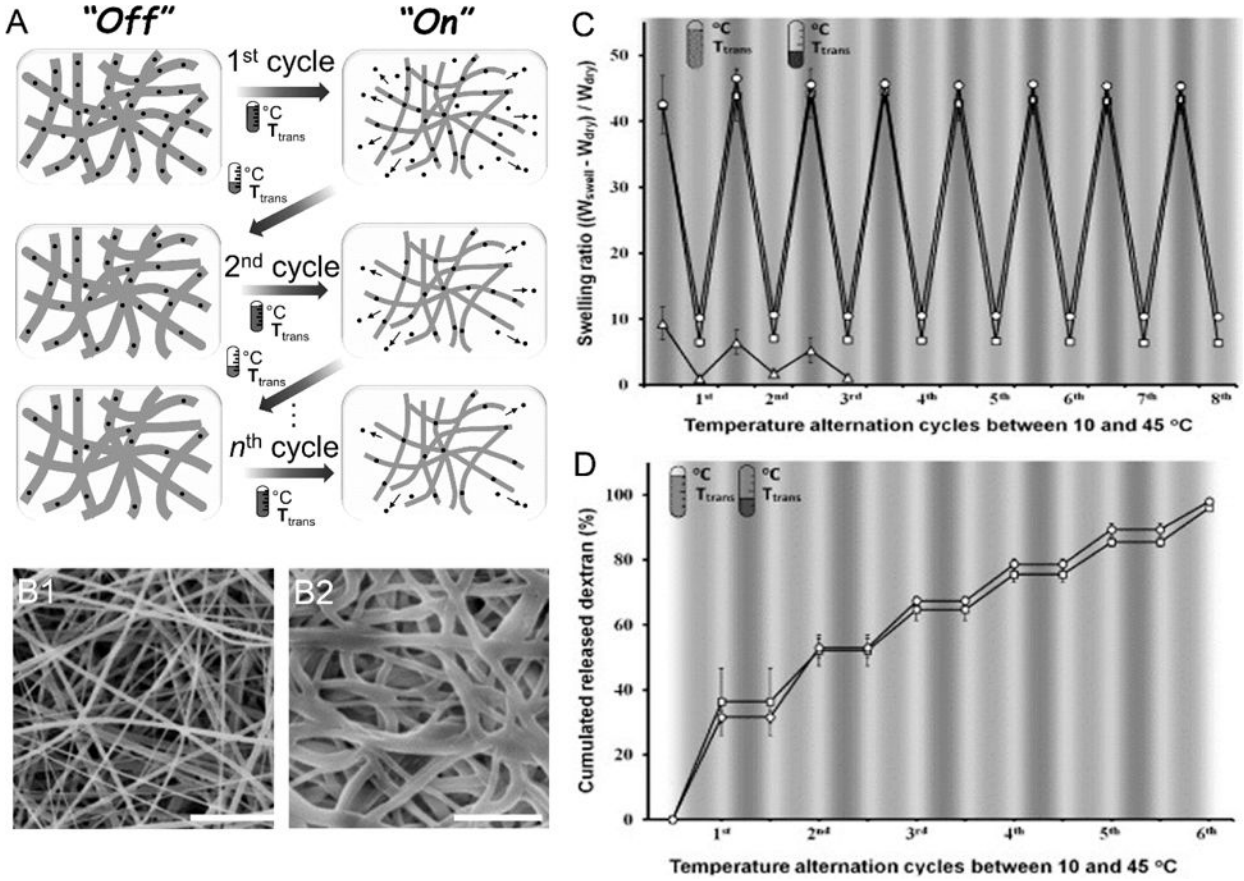

Fig. (7).

(A) Schematic of the "on–off" controlled stepwise release of dextran from P(NIPAAm-*co*-HMAAm) in response to cycles of temperature alternation. (B1) SEM image of PNH_10 after thermal crosslinking at 110 °C for 7 h. (PNH_X is the abbreviation of P(NIPAAm-*co*-HMAAm) (PNH) and mole percent of HMAAm (X) (B2) Cross-linked PNH_10 nanofibers after one cycle of temperature alternation between 10 and 45 °C. The scale bar is 5 μm. (C) Temperature variations of swelling ratio for the cross-linked PNH_3 (Δ), PNH_5 (□) and PNH_10 (○) nanofibers in response to cycles of temperature alternation between 10 and 45 °C. The nanofibers were equilibrated at each temperature for 5 min, and their weights were measured. (D) Release profiles of FITC-dextran from cross-linked PNH_5 and PNH_10 in response to cycles of temperature alternation between 10 and 45 °C. The nanofibers were incubated at each temperature for 5 min and the amounts of released FITC-dextran were measured. (Reprinted from ref. [112])

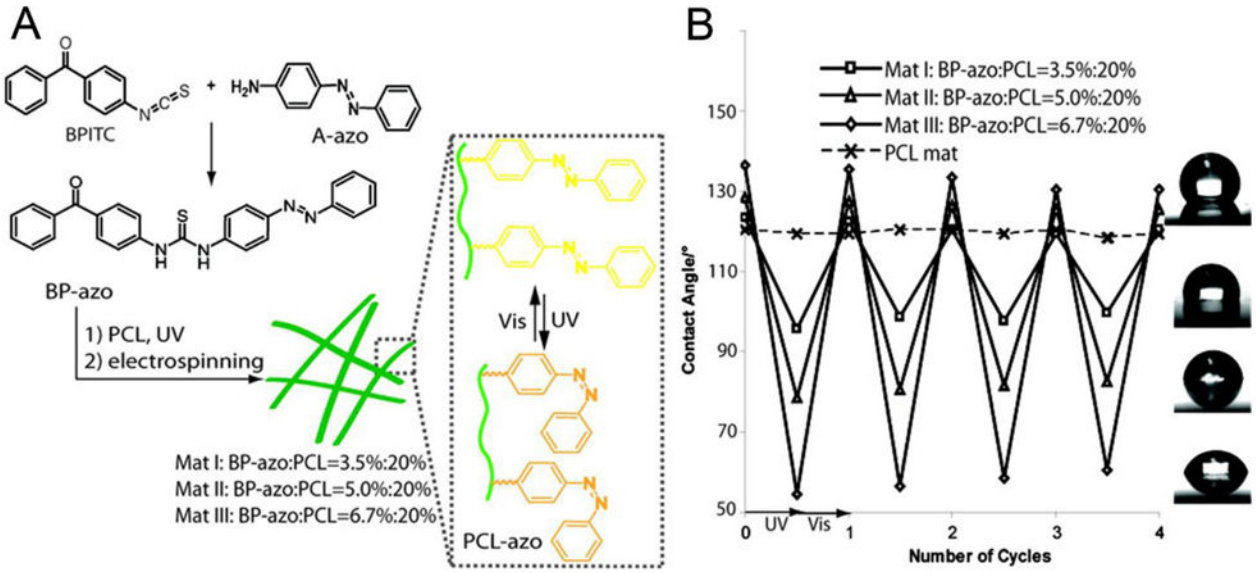

Fig. (8).

(A) Schematic illustration of electrospun PCL-azo nanofibers and the produced light-responsive nanofibers switched “on” and “off” by visible and UV light. (B) The diagram of contact angles dependent on different light radiations shows photoresponsive wettability and the good reversibility of PCL-azo nanofibers. The shapes of water droplets on the mats I–III suggest the hydrophilic nature of PCL-azo is dependent on the amount of added azo. (Reprinted from [130])

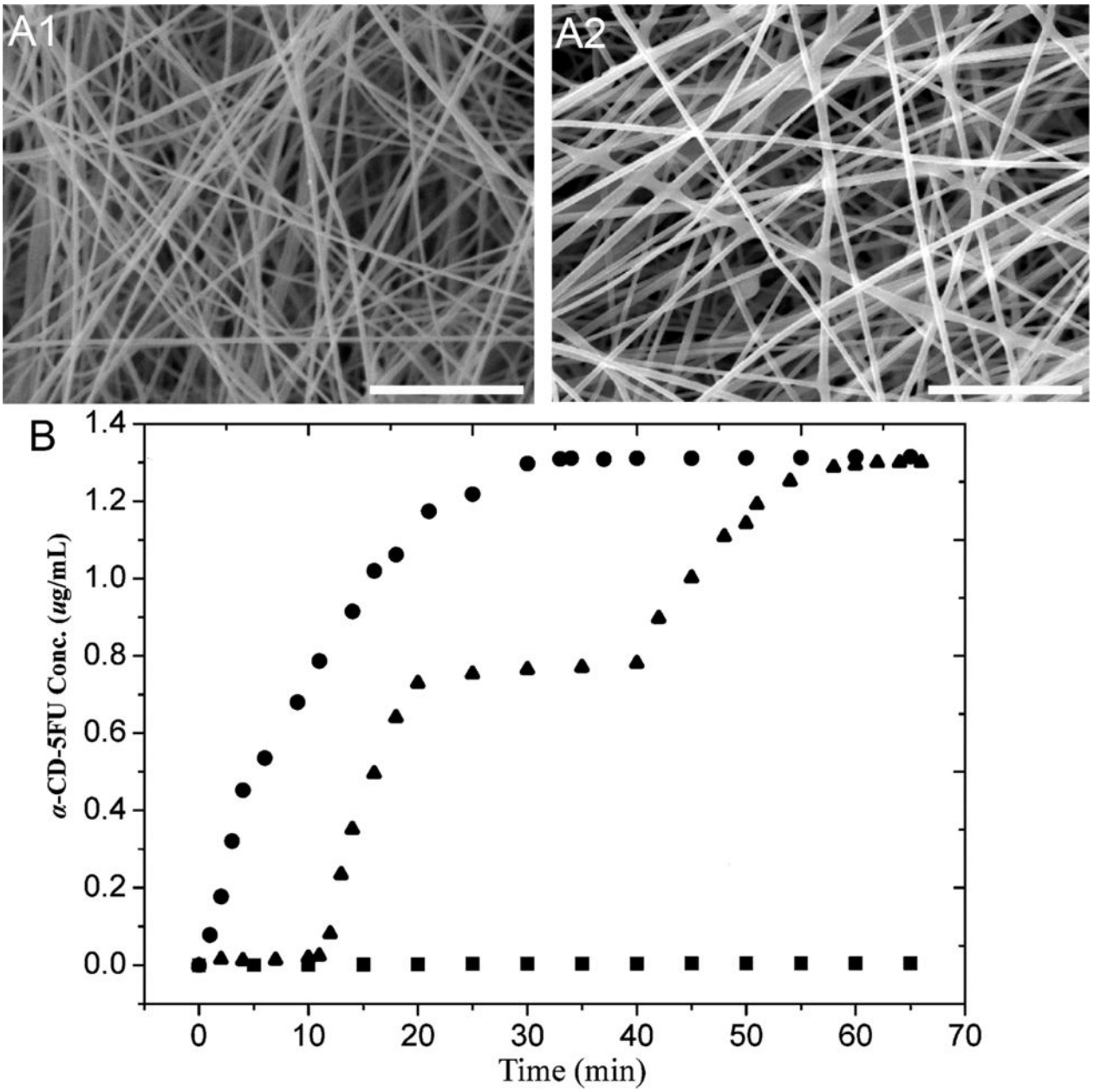

Fig. (9).

SEM images of cross-linked PVBC-*b*-PGMA-azo nanofibers (A1) and the cross-linked PVBC-*b*-PGMA-azo nanofibers after loading and photo-controlled release of α-CD-5FU prodrug (A2). The scale bar is 10 μm. (B) The release profiles of α-CD-5FU prodrug from the synthesized electrospun nanofibers at different light conditions. ■: Dark; ●: continuous exposure to 365 nm UV irradiation; ▲: intermittent exposure to 365 nm UV irradiation in the time interval of 10–20 and 40–70 min. (Reprinted from ref. [131])

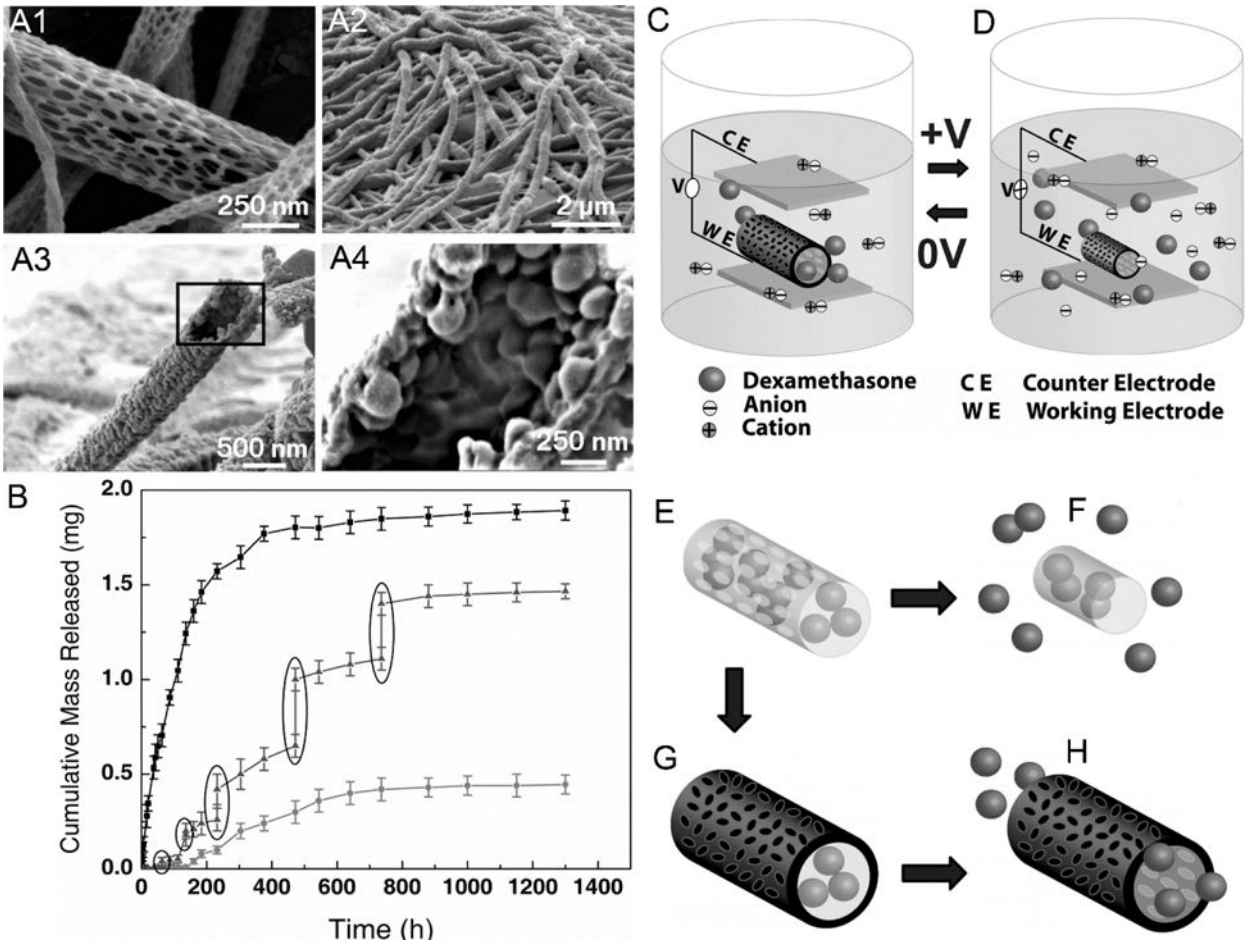

Fig. (10).

SEM images of (A1) PLGA nanofibers, (A2) PEDOT coated PLGA nanofibers, (A3) PEDOT nanotubes after removing PLGA by DCM, and (A4) magnified image of (A3). (B) Cumulative mass release of DEX from: PLGA nanofibers (top line), PEDOT-coated PLGA nanofibers (bottom line) without electrical stimulation, and PEDOT-coated PLGA nanofibers with electrical stimulation of 1 V applied at the five specific times indicated by the circled data points (middle line). (C, D) Schematic illustration of the electrical field induced the release of DEX. Schematic illustration of (E) DEX-loaded electrospun PLGA nanofibers, (F) hydrolytic degradation of PLGA nanofibers leading to the release of DEX, (G) electrochemical deposition of PEDOT on the DEX-loaded electrospun PLGA nanofibers, and (H) the release of DEX from PEDOT-coated and DEX-loaded PLGA nanofibers. (Reprinted from ref.[148])

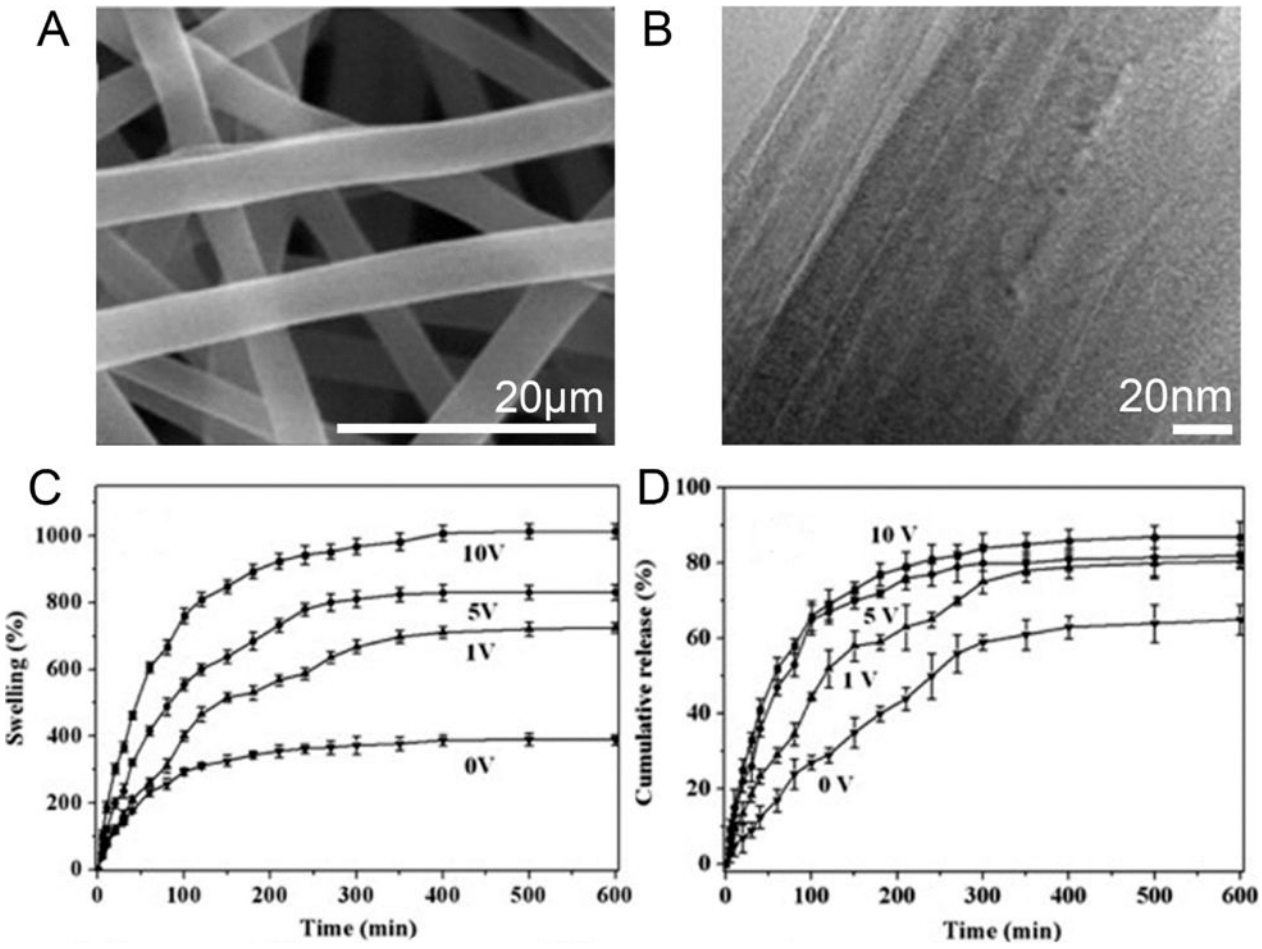

Fig. (11).

SEM (A) and TEM (B) images of OF82F10 nanofibers. The ratio of O_2:F_2 in the oxyfluorination was 8:2 and the wt% of MWCNTs in the membrane was 10%. (C) Swelling behavior of OF82F10 nanofibers at different electric voltages. (D) Drug release profiles from OF82F10 nanofibers at different electric voltages. (Reprinted from ref. [150])

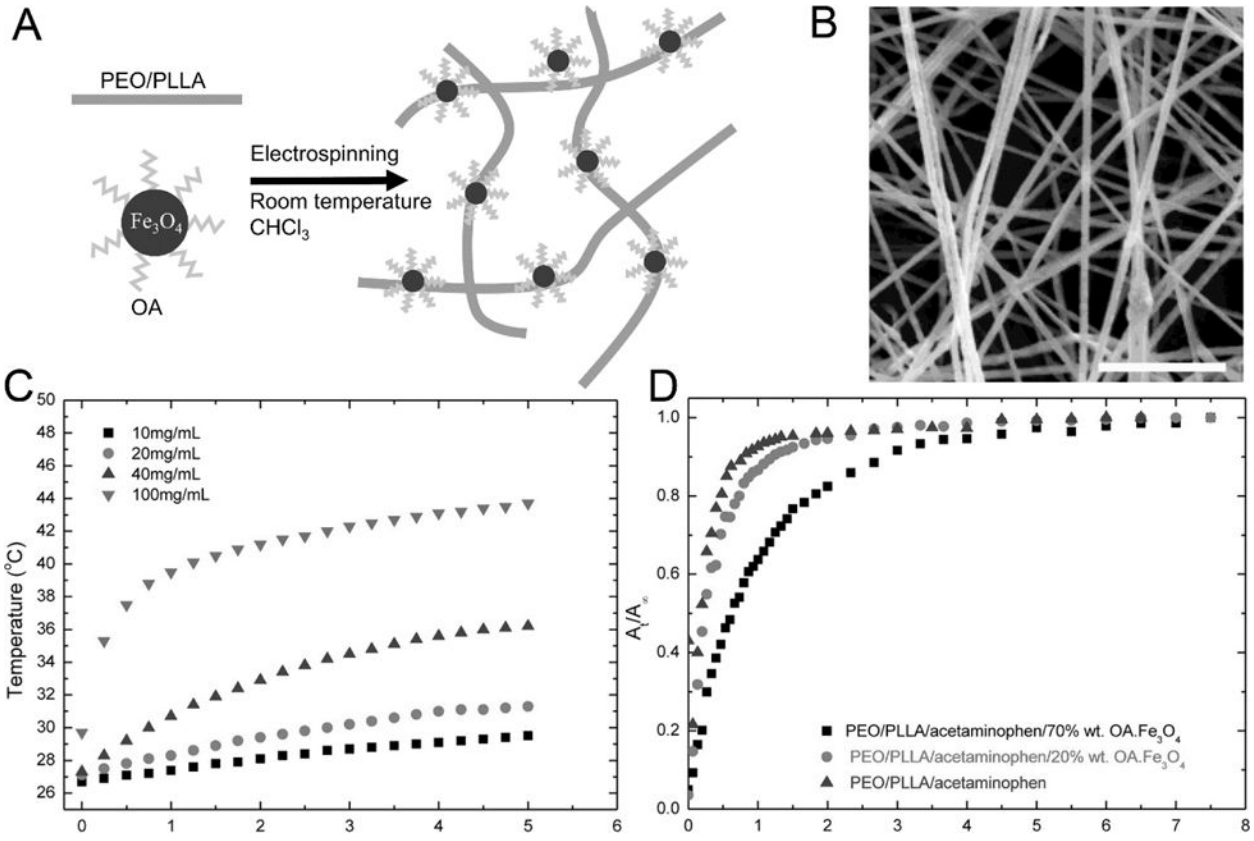

Fig. (12).

(A) Schematic illustrating the preparation of electrospun PEO/PLLA/OA-Fe_3O_4 nanofibers. (B) SEM image of PEO/PLLA/OA-Fe_3O_4 nanofibers with 20% OA-Fe_3O_4 loading. The scale bar is 20 μm. (C) Time-dependent temperature curves of the magnetoactive membranes at different concentrations of Fe_3O_4 at 110 kHz and 25 mT magnetic field. (D) Cumulative percentage release profiles of acetaminophen from PEO/PLLA/acetaminophen fiber samples containing 0, 20, and 70 % OA-Fe_3O_4. (Reprinted from ref. [162])

Table 1

Optimized nanofiber fabrication parameters and their effects on the diameter, morphology, and structure.

Parameters	**Effects on the diameter, morphology, and structure of nanofibers**
Flow rate (Q)↑	Nanofiber diameter↑ (Eventually the continuity of the fiber ceases and it breaks into beads)
Applied high voltage (V)↑	Nanofiber diameter↓, then↑
Distance (D)↑	Nanofiber diameter↓ (Beaded morphology occurs if the distance is too short and the electric field is too strong)
Viscosity of polymer solution (η)↑	Nanofiber diameter↑
Relative volatility of polymer solution (α)↑	Porous microstructure appears due to higher volatility
Conductivity of the solution (σ)↑	Nanofiber diameter↓
Relative humidity(ϕ)↑	Porous microstructure appears due to evaporation-cooling effects and/or phase separation

Table 2

List of temperature sensitive polymers and their LCSTs

Class	Polymer name	LCSTs (°C)	Ref.
Poly(N-alkyl) substituted acrylamides	Poly(N-isopropylacrylamide) (PNIPAAm)	32	[101]
	Poly(N-iso-propylmethacrylamide) (PNIPMAM)	42	[103]
	Poly(N-cyclopropylacrylamide) (PNCPAL)	40–50	[104]
	Poly(N,N-diethylacrylamide) (PDEA)	33	[105]
	PolyN-(2,2-Dimethyl-1,3-dioxan-5-yl)Methacrylamide (PNDMM)	15.3	[106]
	PolyN-(2,2-Dimethyl-1,3-dioxan-5-yl)Acrylamide (PNDMA)	17.8	[106]
Poly(N-vinylalkylamides)	Poly(N-vinylcaprolactam) (PVCL)	32–35	[107]
Polyethers	Poly(methyl vinyl ether) (PMVE)	37	[108]
	Poly(ethylene oxide)–Poly(propylene oxide) (PEO-PPO)	12.5–52.5	[109]